QUANTITATIVE FINANCE
RESEARCH CENTRE

UNIVERSITY OF
TECHNOLOGY SYDNEY

QUANTITATIVE FINANCE RESEARCH CENTRE

Research Paper 304 March 2012

Modelling Default Correlations in a Two-Firm Model with Dynamic Leverage Ratios

Carl Chiarella, Chi-Fai Lo and Ming Xi Huang

ISSN 1441-8010 www.qfrc.uts.edu.au

MODELLING DEFAULT CORRELATIONS IN A TWO-FIRM MODEL WITH DYNAMIC LEVERAGE RATIOS

CARL CHIARELLA[†], CHI-FAI LO[‡] AND MING XI HUANG[⋆]

Abstract. This article provides a generalized two-firm model of default correlation, based on the structural approach that incorporates interest rate risk. In most structural models default is driven by the firms' asset dynamics. In this article, a two-firm model of default is instead driven by the dynamic leverage ratios, which combines the measure of risks of the firms' total liabilities and assets. This article investigates analytical methods and numerical tools to solve the two-dimensional first passage time problem with time-dependent parameters. We carry out a comparative analysis of the impact of model parameters and provide some insights of their effects on joint survival probabilities and default correlations.

Keywords: Credit Risk, Default Correlations, Default Probabilities, First Passage Time

JEL CLASSIFICATION SYSTEM: **C60**, **G13**, **G32**.

1. Introduction

Default correlations have been an important research area in credit risk analysis. There are a number of approaches for credit risk modelling, for example, the Gaussian copula method, the reduced-form approach and the structural approach. In the structural approach, default happens when the firm value falls below a default threshold. For example the fundamental model of Merton (1974) assuming that default could only happen at the maturity date of the bond, was later modified by Black & Cox (1976) to allow default before the maturity date. Longstaff & Schwartz (1995) combine the early default mechanism in Black & Cox (1976)

This version: 22 December 2011

[†]Carl.Chiarella@uts.edu.au; Finance Discipline Group, UTS Business School, University of Technology, Sydney.

[‡]CFLo@phy.cuhk.edu.hk; Institute of Theoretical Physics and Department of Physics, The Chinese University of Hong Kong.

[⋆]Corresponding author: MingXi.Huang@alumni.uts.edu.au; Finance Discipline Group, UTS Business School, University of Technology, Sydney, P.O. Box 123, Broadway NSW 2007, Australia.

and the stochastic interest rate model of Vasicek (1977). Their model also accommodates the complicated liability structures and payoffs by deriving the solution as a function of a ratio of the firm value to the bond payoff value. Instead of using a constant default threshold, Briys & de Varenne (1997) consider a time-dependent default threshold and assume that it depends on the risk-free interest rate.

Later developments by Collin-Dufresne & Goldstein (2001) and Hui, Lo & Huang (2006) consider the stationary leverage ratio for modelling credit risk. Collin-Dufresne & Goldstein (2001) assume that the default threshold changes dynamically over time, in particular, that the dynamics of the log-default threshold is mean-reverting. This setting captures the fact that firms tend to issue debt when their leverage ratios fall below some target, and replace maturing debt when their leverage ratios are above this target. Hui et al. (2006) generalize the Collin-Dufresne & Goldstein (2001) model to consider the situation in which the target leverage ratio is time-dependent. The bond pricing functions in Collin-Dufresne & Goldstein (2001) and Hui et al. (2006) are in terms of the ratio of the default threshold to the firm value. The default threshold is assumed as the total liabilities of the firm. For such a combined measure of the default risk of the firm, Hui, Lo, Huang & Lee (2007) proposed a dynamic leverage ratio model, where default is driven by the firm's leverage ratio when it is above a certain level.

The aim of this article is to extend the dynamic leverage ratio model of Hui et al. (2007) to the two-firm case so as to study the implications for default correlations. The two-firm model has been proposed by Zhou (2001), who extends the one-firm model of Black & Cox (1976) to the two-firm situation. In Zhou (2001) the arrival of the default is driven by firms' asset values and the short-term risk-free interest rate is deterministic. In contrast to Zhou (2001), the arrival of default in the two-firm model in this article is driven by firms' leverage ratios, and the risk-free interest rate is stochastic. We also extend the methods and techniques applied in Hui et al. (2007) for solving the first-passage-time problem in a two-dimensional situation. The third aim of this article is to develop numerical schemes which apply more generally.

The reminder of this article is organized as follows. Section 2 reviews the dynamic leverage ratio model of Hui et al. (2007), and the techniques used in Hui et al. (2007) for solving the first-passage-time problem: the method of images and the time varying barrier technique for dealing

with time-dependent parameters. Section 3 extends the dynamic leverage ratio model to the two-firm situation for valuation of default correlations. Section 4 shows the numerical results of the impact on joint survival probabilities and default correlations for a range of different scenarios, for example, different correlation levels, drift rates, volatilities and initial leverage ratios. Section 5 concludes.

2. **The Hui et al. (2007) Model**

The Hui et al. (2007) model assumes that corporate bond prices depend on a firm's leverage ratio and the risk-free interest rate. The leverage ratio L is assumed the ratio of the firm's total liability to the firm value. The leverage ratio is assumed to follow the geometric Brownian motion

$$dL = \mu_L(t)Ldt + \sigma_L(t)LdZ_L, \tag{1}$$

where $\mu_L(t)$ and $\sigma_L(t)$ are the time dependent drift rate and the volatility of the proportional change in the leverage ratio, respectively and Z_L is a Wiener process under the historical measure $\mathbb{P}$. The dynamics of the risk-free interest rate is assumed to be given by the Hull & White (1990) model, so that

$$dr = \kappa_r(t)\left[\theta_r(t) - r\right]dt + \sigma_r(t)dZ_r, \tag{2}$$

where the risk-free interest r is mean-reverting to the long-run mean $\theta_r(t)$ at speed $\kappa_r(t)$, $\sigma_r(t)$ is the instantaneous volatility of interest rate changes and Z_r is a Wiener process under the historical measure $\mathbb{P}$.

The Wiener increments dZ_L and dZ_r are assumed to be correlated with[1]

$$\mathbb{E}[dZ_L dZ_r] \;=\; \rho_{Lr}(t)dt. \tag{3}$$

In Hui et al. (2007), default occurs when the firm's leverage ratio rises above a predefined level $\widehat{L}$ at anytime during the life of the bond, and bondholders receive nothing upon default.

[1]An explicit expressions of the parameters $\mu_L(t)$, $\sigma_L(t)$ and the correlation coefficient ρ_{Lr} relating these to the firm value, the firm's total liabilities and interest rate processes can be found in Hui et al. (2006).

Otherwise, bondholders receive the par value of the bond at the maturity T. Applying the arbitrage pricing argument, the corporate bond price $P(L,r,t)$ is given by

$$\begin{aligned} -\frac{\partial P}{\partial t} &= \frac{1}{2}\sigma_L^2(t)L^2\frac{\partial^2 P}{\partial L^2} + \widetilde{\mu}_L(t)L\frac{\partial P}{\partial L} + \rho_{Lr}(t)\sigma_L(t)\sigma_r(t)L\frac{\partial^2 P}{\partial L \partial r} \\ &\quad + \frac{1}{2}\sigma_r^2(t)\frac{\partial^2 P}{\partial r^2} + \kappa_r(t)[\widetilde{\theta}_r(t) - r]\frac{\partial P}{\partial r} - rP, \end{aligned} \tag{4}$$

for $t \in (0,T)$, $L \in (0,\widehat{L})$ and subject to the boundary conditions

$$P(L,r,T) = 1,\ P(\widehat{L},r,t) = 0. \tag{5}$$

Here

$$\widetilde{\mu}_L(t) = \mu_L(t) - \lambda_L\sigma_L(t),\ \widetilde{\theta}_r(t) = \theta_r(t) - \frac{\lambda_r\sigma_r(t)}{\kappa_r(t)}, \tag{6}$$

where λ_L and λ_r are the market prices of risk[2] of the leverage ratio and interest rate processes, respectively.

Hui et al. (2007) employed the separation of variables method to simplify the problem (4) by setting

$$P(L,r,t) = B(r,t)\widehat{P}(L,t), \tag{7}$$

where $B(r,t)$ is the risk-free bond price, $\widehat{P}(L,t)$ is a function defined on $L < \widehat{L}$ in a period of T and it satisfies the partial differential equation[3]

$$-\frac{\partial \widehat{P}}{\partial t} = \frac{1}{2}\sigma_L^2(t)L^2\frac{\partial^2 \widehat{P}}{\partial L^2} + [\widetilde{\mu}_L(t) + \rho_{Lr}(t)\sigma_L(t)\sigma_r(t)b(t)]\,L\frac{\partial \widehat{P}}{\partial L}, \tag{8}$$

subject to the boundary conditions

$$\widehat{P}(L,T) = 1,\ \widehat{P}(\widehat{L},t) = 0. \tag{9}$$

[2]There are no explicit expressions of the market prices of risk in Hui et al. (2007), and here we simply assume they are constant.

[3]Note that the fact that the drift of the dynamic leverage ratio does not depend on the risk-free interest rate allows the separation of variables technique to work in this situation. A derivation of (8) can be found in the Appendix of Hui et al. (2007). Under the risk-neutral measure, the growth rates of the firm's asset value and the firm's total liabilities equal the risk-free interest rate, as a result $\widetilde{\mu}_L(t)$ is independent on the risk-free interest rate.

Equation (8) can be transformed further to a simpler form by using the normalized log-leverage ratio $x = \ln(L/\widehat{L})$, and $\tau = T - t$ the time-to-maturity. Set $\widehat{P}(\widehat{L}e^x, t)$ equal to $\bar{P}(x, \tau)$, then $\bar{P}(x, \tau)$ satisfies the partial differential equation

$$\frac{\partial \bar{P}}{\partial \tau} = \frac{1}{2}\sigma_L^2(\tau)\frac{\partial^2 \bar{P}}{\partial x^2} + \gamma(\tau)\frac{\partial \bar{P}}{\partial x}, \tag{10}$$

for $\tau \in (0, T)$, $x \in (\infty, 0)$ and subject to the boundary conditions

$$\bar{P}(x, 0) = 1, \tag{11}$$

$$\bar{P}(0, \tau) = 0, \tag{12}$$

where

$$\gamma(\tau) = \widetilde{\mu}_L(\tau) + \rho_{Lr}(\tau)\sigma_L(\tau)\sigma_r(\tau)b(\tau) - \frac{1}{2}\sigma_L^2(\tau). \tag{13}$$

The its solution can be written as

$$\bar{P}(x, \tau) = \int_{-\infty}^{0} f(x, y; \tau)\bar{P}(y)dy, \tag{14}$$

where $\bar{P}(x, 0) \equiv \bar{P}(y)$ is the initial condition function which is given in (11), $f(x, y; \tau)$ is the transition probability density function for x starting at the value $x(0) = y$ at $\tau = 0$ and ending at the value x at τ, and it is subject to the zero boundary condition in (12).

2.1. *The Method of Images for Constant Coefficients.*

It is the boundary condition (12) that gives defaultable bond pricing problems its particular structure and difficulty. This is essentially a barrier type condition and in one form or another requires the solution of the first passage time[4] problem associated with the partial differential equation (10). To solve this type of problem, Hui et al. (2007) apply the method of images approach. When the model parameters are constant and $\rho_{Lr} = 0$, that is $\sigma_L(\tau) = \sigma_L$ and

[4]In statistics, the first passage time is the time when a stochastic process first enters a threshold state. Here the first passage time is the first time x crosses the barrier at $x = 0$.

$\gamma(\tau) = \gamma$, the exact solution of the transition probability density function is[5]

$$f(x, y; \tau) = \exp\Big\{ -\frac{\gamma}{\sigma_L^2}(x - y) - \frac{\gamma^2}{2\sigma_L^2}\tau \Big\} \Big[g(x, y; \sigma_L^2\tau) - g(x, -y; \sigma_L^2\tau) \Big], \tag{15}$$

where

$$g(x, y; v) = \frac{e^{-(x-y)^2/2v}}{\sqrt{2\pi v}}. \tag{16}$$

Albanese & Campolieti (2006) use an alternative approach of the reflection principle to obtain the transition probability density function, and show that it is indeed the same transition probability density function for the survival probability for the absorption not yet having occurred during a period of time $\xi = t - t_0$, that is

$$F(x, \xi) = \int_{-\infty}^{0} f(x, y; \sigma_L^2\xi) dy. \tag{17}$$

2.2. *The Method of Images for Time Varying Coefficients.*

If the coefficients in the partial differential equation (10) are time-dependent, the application of the method of images will not be as straight forward as in the constant coefficients case. Indeed, the exact solution $\bar{P}(x, \tau)$ cannot be solved by applying the method of images, instead, an approximate solution can be obtained. Hui et al. (2007) apply a simple approach that was developed by Lo, Lee & Hui (2003) to construct an approximate solution, namely $\bar{P}_\beta(x, \tau)$, which satisfies the partial differential equation (10) and subject to the initial condition (11). The approach of Lo et al. (2003) is to set the zero boundary condition of $\bar{P}_\beta(x, \tau)$ at a time varying barrier, namely $x^*(\tau)$, which is along the normalized log-leverage ratio x-axis, that is

$$\bar{P}_\beta(x^*(\tau), \tau) = 0. \tag{18}$$

The dynamic form of $x^*(\tau)$ is assumed to be

$$x^*(\tau) = -\int_0^\tau \gamma(v) dv - \beta \int_0^\tau \sigma_L^2(v) dv, \tag{19}$$

[5]See Appendix A for the proof.

where β is a real parameter, which may be chosen in some optimal way so as to minimize the deviation between the time varying barrier $x^*(\tau)$ and the exact barrier at $x = 0$.

By applying the method of images, the approximate solution is

$$\bar{P}_\beta(x,\tau) = \int_{-\infty}^{0} f_\beta(x,y;\tau)\bar{P}_\beta(y)dy, \tag{20}$$

where $\bar{P}_\beta(y) = 1$ at $\tau = 0$ is the initial condition, and $f_\beta(x,y;\tau)$ is the transition probability density function for the process restricted to the region $x \in (-\infty, x^*(\tau))$ and has the form[6]

$$\begin{aligned} f_\beta(x,y,\tau) &= \exp\Big\{\beta\big[x-y-x^*(\tau)\big] - \frac{1}{2}\beta^2\int_0^\tau \sigma_L^2(v)dv\Big\} \\ &\quad \times\Big[g\Big(x-x^*(\tau), y; \int_0^\tau \sigma_L^2(v)dv\Big) - g\Big(x-x^*(\tau), -y; \int_0^\tau \sigma_L^2(v)dv\Big)\Big]. \end{aligned} \tag{21}$$

The survival probability for the absorption not yet having occurred during a period of time $\xi = t - t_0$ is thus

$$F_\beta(x,\xi) = \int_{-\infty}^{0} f_\beta(x,y;\xi)dy. \tag{22}$$

Note that the accuracy of the approximate solution depends on choosing the values of β. Lo et al. (2003) illustrate certain forms of β that provide accurate results, for example by setting $x^*(0) = x^*(T) = 0$. A particular form of β can be obtained according to (19), so that

$$\beta = -\frac{\int_0^T \gamma(v)dv}{\int_0^T \sigma_L^2(v)dv}. \tag{23}$$

Other methodologies of choosing the optimal values of β are discussed in Lo et al. (2003).

3. **Modelling Default Correlations in A Two-Firm Model**

3.1. *Default Correlations.*

[6]See Appendix B for the proof.

Default correlation measures the likelihood of firms defaulting together. The mathematical interpretation of default correlation by Zhou (2001) is

$$\rho_D = \frac{\text{JPD} - \text{PD}_1\text{PD}_2}{\sqrt{\text{PD}_1(1-\text{PD}_1)}\sqrt{\text{PD}_2(1-\text{PD}_2)}}, \tag{24}$$

where JPD is the joint default probability of the two firms $i = 1, 2$ and PD_i are individual default probabilities of the two firms.

Default correlation in (24) can be explained as the normalized difference between both firms default at the same time when they are correlated and both firms default at the same time when they are uncorrelated.

To solve (24), individual default probabilities can be obtained by solving equations (17) and (22). The JPD can be expressed in terms of joint survival probability, JSP according to

$$\text{JPD} = \text{JSP} - 1 + \text{PD}_1 + \text{PD}_2, \tag{25}$$

where JSP will be determined in the following section.

3.2. *A Two-Firm Model with Dynamic Leverage Ratios.*

To valuate the joint survival probability of two firms, we consider a financial instrument - credit linked note (CLN) that it exposed to the default risk of the note issuer and the reference asset. A credit linked note allows the issuer to transfer the credit risk of holding a bond to the investors. If the bond issuer (or the"reference obligor") is solvent, the note issuer is obligated to pay to the note-holders the note face value at the maturity. If the reference obligor goes bankrupt, the note-holders receive a recovery rate or in the worst case they receive nothing. The note-holders are also exposed to the default risk of the note issuer. Therefore, the price of the note is linked to the performance of the reference asset and the default risk of the note issuer. To model the CLN, we extend the Hui et al. (2007) dynamic leverage ratio model to the two firm situation and incorporate the stochastic risk-free interest rate.

Let L_1 and L_2 denote respectively the leverage ratios of the note issuer and the reference obligor, and assume that they follow the dynamics

$$dL_i = \mu_i L_i dt + \sigma_i L_i dZ_i, \ (i = 1, 2), \tag{26}$$

where μ_i and σ_i denote the constant drift rate and volatility of the proportional change in leverage ratios respectively, and Z_1 and Z_2 are Wiener processes under the historical measure $\mathbb{P}$. The Wiener increments dZ_1 and dZ_2 are assumed to be correlated with

$$\mathbb{E}[dZ_1 dZ_2] = \rho_{12} dt, \tag{27}$$

where ρ_{12} denotes the correlation coefficient of the proportional leverage ratio level of the two firms.

Let the dynamics of the instantaneous spot rate of interest follow the Vasicek (1977) process

$$dr = \kappa_r (\theta_r - r) dt + \sigma_r dZ_r, \tag{28}$$

where the instantaneous spot rate of interest r is mean-reverting to the constant long-term mean θ_r at constant speed κ and Z_r is a Wiener process under the historical measure $\mathbb{P}$. The Wiener processes Z_i and Z_r are correlated with

$$\mathbb{E}[dZ_i dZ_r] = \rho_{ir} dt, \ (i = 1, 2), \tag{29}$$

where ρ_{ir} denotes the correlation coefficient between the proportional changes of the leverage ratio level of firm i and the instantaneous spot rate of interest.

Assume default(s) occur anytime during the life of the credit linked note when either firm's leverage ratio rises above a predefined default threshold $\widehat{L}_i$, that is $L_i \geq \widehat{L}_i$. If both firms' leverage ratios never reach $\widehat{L}_i$, the note holder receives the face value, which is assumed equal to unity. If default occurs, the firm defaults on all of its obligations immediately, and the note holder receives nothing (that is there is no recovery) upon default of either firm[7].

[7]There could be a recovery payment if the default event happens. However, the assumption of zero recovery captures the worst situation in which investors lose all their investment on credit linked notes. The framework can easily be adjusted to handle the case of some residual recovery rate.

Let $P(L_1, L_2, r, t)$ be the price of credit linked note and applying the arbitrage pricing argument, the partial differential equation for the price is given by

$$\begin{aligned} -\frac{\partial P(L_1,L_2,r,t)}{\partial t} &= \frac{1}{2}\sigma_1^2 L_1^2 \frac{\partial^2 P}{\partial L_1^2} + \frac{1}{2}\sigma_2^2 L_2^2 \frac{\partial^2 P}{\partial L_2^2} + \frac{1}{2}\sigma_r^2 \frac{\partial^2 P}{\partial r^2} + \rho_{12}\sigma_1\sigma_2 L_1 L_2 \frac{\partial^2 P}{\partial L_1 \partial L_2} \\ &\quad + \rho_{1r}\sigma_1\sigma_r L_1 \frac{\partial^2 P}{\partial L_1 \partial r} + \rho_{2r}\sigma_2\sigma_r L_2 \frac{\partial^2 P}{\partial L_2 \partial r} \\ &\quad + \widetilde{\mu}_1 L_1 \frac{\partial P}{\partial L_1} + \widetilde{\mu}_2 L_2 \frac{\partial P}{\partial L_2} + \kappa_r[\widetilde{\theta}_r - r]\frac{\partial P}{\partial r} - rP. \end{aligned} \tag{30}$$

on the interval $L_i \in (0, \widehat{L}_i)$ (i=1,2), $t \in (0, T)$ and subject to the boundary conditions

$$P(L_1, L_2, r, T) = 1, \tag{31}$$

$$P(\widehat{L}_1, L_2, r, t) = 0, \tag{32}$$

$$P(L_1, \widehat{L}_2, r, t) = 0. \tag{33}$$

The parameters $\widetilde{\mu}_i$ and $\widetilde{\theta}_r$ incorporate the market prices of risk, λ_i, λ_r (assumed to be constant), associated with leverage ratios and interest rate processes respectively and are defined as

$$\widetilde{\mu}_i = \mu_i - \lambda_i\sigma_i, \ (i = 1, 2), \tag{34}$$

$$\widetilde{\theta}_r = \theta_r - \frac{\lambda_r\sigma_r}{\kappa_r}. \tag{35}$$

Extending the method of separation of variables used in Hui et al. (2007) to the two-firm case, we seek to express the credit linked note price in the separable form

$$P(L_1, L_2, r, t) = B(r, t)\widehat{P}(L_1, L_2, t), \tag{36}$$

where $B(r, t)$ is the risk-free bond price, and $\widehat{P}(L_1, L_2, t)$ satisfies

$$\begin{aligned} -\frac{\partial \widehat{P}}{\partial t} &= \frac{1}{2}\sigma_1^2 L_1^2 \frac{\partial^2 \widehat{P}}{\partial L_1^2} + \rho_{12}\sigma_1\sigma_2 L_1 L_2 \frac{\partial^2 \widehat{P}}{\partial L_1 \partial L_2} + \frac{1}{2}\sigma_2^2 L_2^2 \frac{\partial^2 \widehat{P}}{\partial L_2^2} \\ &\quad + [\widetilde{\mu}_1 + \rho_{1r}\sigma_1\sigma_r b(t)]\, L_1 \frac{\partial \widehat{P}}{\partial L_1} + [\widetilde{\mu}_2 + \rho_{2r}\sigma_2\sigma_r b(t)]\, L_2 \frac{\partial \widehat{P}}{\partial L_2}, \end{aligned} \tag{37}$$

subject to the boundary conditions

$$\widehat{P}(L_1, L_2, T) = 1, \tag{38}$$

$$\widehat{P}(\widehat{L}_1, L_2, t) = 0, \tag{39}$$

$$\widehat{P}(L_1, \widehat{L}_2, t) = 0. \tag{40}$$

In (37) $b(t)$ is a time-dependent parameter depending on the speed of mean reversion of the spot rate of interest given by

$$b(t) = \frac{e^{-\kappa_r(T-t)} - 1}{\kappa_r}. \tag{41}$$

Define the volatility adjusted log-leverage ratios

$$X_i = \ln(L_i/\widehat{L}_i)/\sigma_i, \tag{42}$$

and denote $\widehat{P}(\widehat{L}_1 e^{\sigma_1 X_1}, \widehat{L}_2 e^{\sigma_2 X_2}, t)$ by $\bar{P}(X_1, X_2, \tau)$, so that in terms of time-to-maturity variable $\tau = T - t$, the partial differential equation (37) becomes

$$\frac{\partial \bar{P}}{\partial \tau} = \frac{1}{2}\frac{\partial^2 \bar{P}}{\partial X_1^2} + \rho_{12}\frac{\partial^2 \bar{P}}{\partial X_1 \partial X_2} + \frac{1}{2}\frac{\partial^2 \bar{P}}{\partial X_2^2} + \gamma_1(\tau)\frac{\partial \bar{P}}{\partial X_1} + \gamma_2(\tau)\frac{\partial \bar{P}}{\partial X_2}, \tag{43}$$

on the interval of $X_i \in (-\infty, 0)$ (i=1,2), $\tau \in (0, T)$ and subject to the boundary conditions with a new notation that $X_i(0) = Y_i$ (i=1,2) at time-to-maturity $\tau = 0$

$$\bar{P}(Y_1, Y_2) \equiv \bar{P}(X_1, X_2, 0) = 1, \tag{44}$$

$$\bar{P}(0, X_2, \tau) = 0, \tag{45}$$

$$\bar{P}(X_1, 0, \tau) = 0. \tag{46}$$

The drift coefficients $\gamma_i(\tau)$ in (43) are defined as

$$\gamma_i(\tau) = [\widetilde{\mu}_i + \rho_{ir}\sigma_i\sigma_r b(\tau) - \sigma_i^2/2]/\sigma_i, \ (i = 1, 2). \tag{47}$$

The solution to the partial differential equation (43) is given by the integral

$$\bar{P}(X_1, X_2, \tau) = \int_{-\infty}^{0}\int_{-\infty}^{0} f(X_1, X_2, Y_1, Y_2; \tau)\bar{P}(Y_1, Y_2)dY_1 dY_2, \tag{48}$$

where $f(X_1, X_2, Y_1, Y_2; \tau)$ is the transition probability density function for transition from the values $X_1(0) = Y_1$ and $X_1(0) = Y_2$ at time-to-maturity $\tau = 0$ below the barriers to the values X_1 and X_2 at time-to-maturity τ within the region $X_1 \in (-\infty, 0)$ and $X_2 \in (-\infty, 0)$.

3.3. *Method of Images for Constant Coefficients at Certain Values of ρ_{12}.*

The zero boundary conditions in (45)-(46) requires the solution of the first passage time problem[8] associated with the partial differential equation (43). To solve this problem, Appendix Cextends the method of images to the two-dimensional heat equation when it is subject to zero boundary conditions. In order to apply the solution in Appendix C, we assume that the partial differential equation (43) has constant coefficients, that is we set $\rho_{ir} = 0$, then drift terms are no longer time-dependent, that is

$$\gamma_i = [\widetilde{\mu}_i - \sigma_i^2/2]/\sigma_i, \ (i = 1, 2). \tag{49}$$

Next, we transform the partial differential equation (43) with constant coefficients to the two-dimensional heat equation as illustrated in Appendix D. The exact solution for the transition probability density function f is thus given by

$$\begin{aligned} f(X_1, X_2, Y_1, Y_2; \tau) &= \exp\Big\{\eta_1(X_1 - Y_1) + \eta_2(X_2 - Y_2) + \xi\tau\Big\} \\ &\quad \times\Big[g(X_1, X_2, Y_1, Y_2; \tau) + \sum_{k=1}^{m}(-1)^k g^k(X_1, X_2, Y_1^k, Y_2^k; \tau)\Big], \end{aligned} \tag{50}$$

where g is the bivariate transition probability density function for transition from y_1, y_2 to x_1, x_2 in time period τ, and has the form

$$\begin{aligned} &g(x_1, x_2, y_1, y_2; \tau) \\ &= \frac{1}{2\pi\tau\sqrt{1-\rho_{12}^2}}\exp\left\{-\frac{(x_1 - y_1)^2 - 2\rho_{12}(x_1 - y_1)(x_2 - y_2) + (x_2 - y_2)^2}{2\tau(1-\rho_{12}^2)}\right\}, \end{aligned} \tag{51}$$

[8]Here the first passage time is the first time X_i (i=1,2) crosses the barrier at $X_i = 0$.

with

$$\eta_1 = \frac{\gamma_2\rho_{12}-\gamma_1}{1-\rho_{12}^2},\ \eta_2 = \frac{\gamma_1\rho_{12}-\gamma_2}{1-\rho_{12}^2}, \tag{52}$$

$$\xi = -\frac{\left(\frac{1}{2}\gamma_1^2-\rho_{12}\gamma_1\gamma_2+\frac{1}{2}\gamma_2^2\right)}{1-\rho_{12}^2}. \tag{53}$$

Note that g^k is equivalent to g, the superscript representing the bivariate transition probability density function obtained from the kth image by the method of images approach.

Here m is the total number of images used to form a closed-loop in such a way that the desired boundary conditions at $X_1 = 0$ and $X_2 = 0$ are preserved, as explained in Appendix D . The Y_1^k and Y_2^k are obtained recursively from the relations between successive images

$$Y_1^k = \begin{cases} -Y_1^{k-1} & \text{for odd } k, \\ Y_1^{k-1}-2\rho_{12}Y_2^{k-1} & \text{for even } k, \end{cases} \tag{54}$$

$$Y_2^k = \begin{cases} Y_2^{k-1}-2\rho_{12}Y_1^{k-1} & \text{for odd } k\ , \\ -Y_2^{k-1} & \text{for even } k\ , \end{cases} \tag{55}$$

where

$$Y_1^1 = -Y_1,\ Y_2^1 = Y_2-2\rho_{12}Y_1. \tag{56}$$

Denote $F(X_1, X_2, \xi)$ by the joint survival probability of absorption not yet having occurred during a period of time $\xi = t - t_0$, that is

$$F(X_1, X_2, \xi) = \int_{-\infty}^{0}\int_{-\infty}^{0} f(X_1, X_2, Y_1, Y_2; \xi)dY_1dY_2, \tag{57}$$

where $f(X_1, X_2, Y_1, Y_2; \xi)$ satisfies the same partial differential equation of $\bar{P}$ as in (43). Note that the solution (50) is obtained by applying the method of images and is valid for the values of ρ_{12} given in Table 1, see Appendix E for the proof.

3.4. *Method of Images for Time Varying Coefficients at Certain Values of ρ_{12}.*

If the coefficients in the partial differential equation (43) are time-dependent, we extend the approach of Lo et al. (2003) discussed in Subsection 2.2 to the two-firm case. Denote by $\bar{P}_{\boldsymbol{\beta}}$

Total no. of images m	ρ_{12}	Values of ρ_{12}
3	$-\cos\frac{\pi}{2}$	0
5	$-\cos\frac{\pi}{3}$	-0.5
7	$-\cos\frac{\pi}{4}$	-0.707
9	$-\cos\frac{\pi}{5}$	-0.809
:	:	:
13	$-\cos\frac{\pi}{7}$	-0.901
:	:	:
m	$-\cos\frac{2\pi}{(m+1)}$	:

TABLE 1. The relation between the number of images m required to form the "closed-loop" and the corresponding value of ρ_{12}.

the approximate solution to the exact solution $\bar{P}$ of the partial differential equation (43) and satisfing the same partial differential equation, that is

$$\frac{\partial \bar{P}_{\boldsymbol{\beta}}}{\partial \tau} = \frac{1}{2}\frac{\partial^2 \bar{P}_{\boldsymbol{\beta}}}{\partial X_1^2} + \rho_{12}\frac{\partial^2 \bar{P}_{\boldsymbol{\beta}}}{\partial X_1 \partial X_2} + \frac{1}{2}\frac{\partial^2 \bar{P}_{\boldsymbol{\beta}}}{\partial X_2^2} + \gamma_1(\tau)\frac{\partial \bar{P}_{\boldsymbol{\beta}}}{\partial X_1} + \gamma_2(\tau)\frac{\partial \bar{P}_{\boldsymbol{\beta}}}{\partial X_2}. \tag{58}$$

The zero boundary conditions $\bar{P}_{\boldsymbol{\beta}}$ are assumed to be

$$\bar{P}_{\boldsymbol{\beta}}(X_1^*(\tau), X_2, \tau) = 0, \tag{59}$$

$$\bar{P}_{\boldsymbol{\beta}}(X_1, X_2^*(\tau), \tau) = 0, \tag{60}$$

where $X_1^*(\tau)$ and $X_2^*(\tau)$ are time varying barriers along the X_1-axis and X_2-axis respectively. Now X_1 and X_2 are restricted to the region $X_1 \in (-\infty, X_1^*(\tau))$ and $X_2 \in (-\infty, X_2^*(\tau))$. Applying a similar approach as in Subsection 2.2, the time varying barriers are given by

$$X_i^*(\tau) = -\int_0^\tau \gamma_i(v)dv - \beta_i \tau, \ (i = 1, 2). \tag{61}$$

Two real adjustable constants β_1 and β_2 control the shape of the time varying barriers $X_1^*(\tau)$ and $X_2^*(\tau)$ and are chosen so that they remains as close as possible to the exact barrier $X_1 = 0$ and $X_2 = 0$ respectively.

The solution for $\bar{P}_{\boldsymbol{\beta}}$ can be written as

$$\bar{P}_{\boldsymbol{\beta}}(X_1, X_1, \tau) = \int_{-\infty}^0 \int_{-\infty}^0 f_\beta(X_1, X_2, Y_1, Y_2; \tau)\bar{P}_{\boldsymbol{\beta}}(Y_1, Y_2)dY_1 dY_2, \tag{62}$$

where $\bar{P}_{\boldsymbol{\beta}}(Y_1, Y_2) = 1$ at $\tau = 0$ is the initial condition, and $f_\beta(X_1, X_2, Y_1, Y_2; \tau)$ is the joint transition probability density function for the processes restricted to the region $X_i \in (-\infty, X_i^*(\tau))$ (i=1,2) and has the form

$$f_\beta(X_1, X_2, Y_1, Y_2; \tau) =$$
$$e^{\bar{\eta}_1[X_1 - X_1^*(\tau) - Y_1] + \bar{\eta}_2[X_2 - X_2^*(\tau) - Y_2] + \bar{\xi}\tau} \Big[g(X_1 - X_1^*(\tau), X_2 - X_2^*(\tau), Y_1, Y_2; \tau)$$
$$+ \sum_{k=1}^{m} (-1)^k g^k(X_1 - X_1^*(\tau), X_2 - X_2^*(\tau), Y_1^k, Y_2^k; \tau) \Big], \tag{63}$$

where $\bar{\eta}_1$, $\bar{\eta}_2$ and $\bar{\xi}$ are constants given by (see Appendix F for the proof.)

$$\bar{\eta}_1 = \frac{-\beta_2\rho_{12} + \beta_1}{1 - \rho_{12}^2},\ \bar{\eta}_2 = \frac{-\beta_1\rho_{12} + \beta_2}{1 - \rho_{12}^2}, \tag{64}$$

$$\bar{\xi} = -\frac{\frac{1}{2}\beta_1^2 - \rho_{12}\beta_1\beta_2 + \frac{1}{2}\beta_1^2}{1 - \rho_{12}^2}. \tag{65}$$

Then the corresponding joint survival probability $F_\beta(X_1, X_2, \xi)$ for absorption has not yet occurred during the period of time $\xi = t - t_0$, is given by

$$F_\beta(X_1, X_2, \xi) = \int_{-\infty}^{0} \int_{-\infty}^{0} f_\beta(X_1, X_2, Y_1, Y_2; \xi) dY_1 dY_2. \tag{66}$$

We note that the solutions (57) and (66) can be expressed in terms of the cumulative bivariate normal distribution function $N_2(\cdot)$. Appendix G of Chiarella, Lo & Huang (2012) illustrates the implementation of (57) and (66) in terms of $N_2(\cdot)$, where the computation of the joint survival probabilities is done in efficient and accurate way. A range of different analytical approximate methods have been proposed for the evaluation of $N_2(\cdot)$. In this article, we apply the widely cited Drezner (1978) method, which is based on direct computation of the double integral by the Gauss quadrature method[9].

We emphasize that the solutions (50) and (63) obtained by applying method of images are only valid for the particular values of the correlation coefficient ρ_{12} shown in Table 1. In the next subsection we will develop numerical methods to solve the problem for all values of ρ_{12}.

[9]For more details of this method and a comparison of speed and accuracy to other approximate methods, see Agca & Chance (2003).

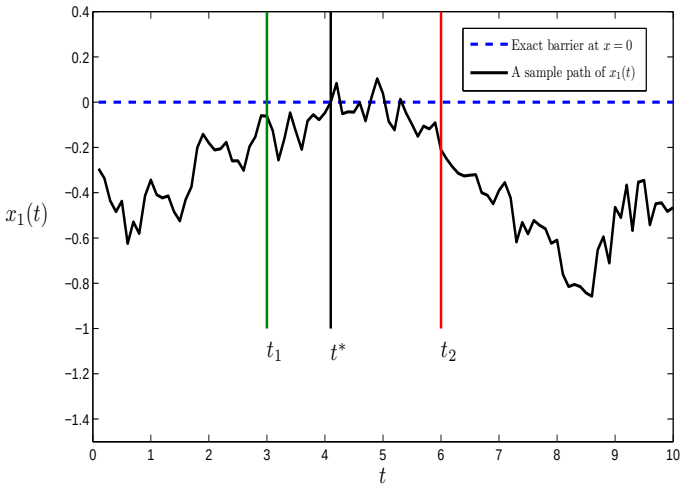

FIGURE 1. A path of $x_1(t)$ across a typical subintervals.

3.5. *Alternative Methodologies for General Values of* ρ_{12}.

We apply the alternating direction implicit method for two-dimensional partial differential equations. We consider the partial differential equation (43), which has a cross-derivative term and time-dependent drift terms. In order to develop an efficient numerical solution, we consider alternating direction implicit (ADI) schemes that are unconditionally stable, that is the they are stable without any restriction on the time step. A recent study conducted by in't Hout & Welfert (2007) showed that the finite difference schemes introduced by Douglas & Rachford (1956) is unconditionally stable in applications to two-dimensional partial differential equation equations with a cross-derivative term and drift terms. Therefore, we apply this scheme to solve the partial differential equation (43). An outline of the scheme is in Appendix I.

We also develop a Monte Carlo (MC) scheme as a benchmark. Consider the partial differential equation (43), then by Feynman-Kac formula, the associated linked stochastic differential equations are

$$dL_1 = [\widetilde{\mu}_1 + \rho_{1r}\sigma_1\sigma_r b(t)]\, L_1 dt + \sigma_1 L_1 d\widetilde{Z}_1, \tag{67}$$

$$dL_2 = [\widetilde{\mu}_2 + \rho_{2r}\sigma_2\sigma_r b(t)]\, L_2 dt + \sigma_2 L_2 d\widetilde{Z}_2, \tag{68}$$

where $\widetilde{Z}_1$ and $\widetilde{Z}_2$ are Wiener processes under the risk-neutral measure $\widetilde{\mathbb{P}}$, and the Wiener increments $d\widetilde{Z}_1$ and $d\widetilde{Z}_2$ are correlated with $\mathbb{E}[d\widetilde{Z}_1 d\widetilde{Z}_2] = \rho_{12}dt$.

We rewrite (67) and (68) in terms of uncorrelated Wiener processes W_1, W_2, and change variables to the normalized log-leverage ratios $x_i = ln(L_i/\widehat{L}_i)$, then (67) and (68) become

$$dx_1 = \left[\widetilde{\mu}_1 + \rho_{1r}\sigma_1\sigma_r b(t) - \frac{1}{2}\sigma_1^2\right] dt + \sigma_1 dW_1, \tag{69}$$

$$dx_2 = \left[\widetilde{\mu}_2 + \rho_{2r}\sigma_2\sigma_r b(t) - \frac{1}{2}\sigma_2^2\right] dt + \sigma_2\big(\rho_{12}dW_1 + \sqrt{1-\rho_{12}^2}dW_2\big). \tag{70}$$

Default occurs any time in the time interval $t \in (0, T)$ if either firm's leverage ratio L_i is on or above the default threshold $\widehat{L}_i$ (that is $x_1 \geq 0$ or $x_2 \geq 0$). Therefore, to ensure that default events are captured, the simulation time step Δt should be as small as possible. For example, Figure 1 shows that, if $\Delta t = t_2 - t_1$, and the barrier is breached at $t^*(t_1 < t^* < t_2)$ the default event will not be captured, and, a smaller $\Delta t = t^* - t_1$ would be required. The details of the Monte Carlo scheme for valuation the joint survival probability are discussed in Appendix J.

4. **Numerical Results**

This section will show some numerical results on joint survival probabilities, default correlations and the price of the credit linked note. We choose the set of parameters to be consistent with Hui et al. (2007), so allowing us to compare the effect of going from a one-firm model to a two-firm model. It is quite natural to set the default threshold at $\widehat{L}_1 = \widehat{L}_2 = 1$, to reflect the fact that the firm's debt level is equal to its asset level. This is equivalent to what is done by Collin-Dufresne & Goldstein (2001) where default occurs when the log-leverage ratio hits the barrier at zero. A firm can be also forced to default when its debt level is close to its asset level, for example 90% ($\widehat{L}_i = 0.9$), or higher than its asset level at 110% ($\widehat{L}_i = 1.1$). However the framework of the two-firm model can handle these more general situations, because the model is formulated in terms of the normalized log-leverage ratios, i.e. $\ln(L_i/\widehat{L}_i)$.

The leverage ratios used for different individual ratings are the typical values of industry medians given by Standard & Poors (2001). Following the same setting in Hui et al. (2007), the values of the volatility of leverage ratios are assumed to be similar to asset volatilities[10], the

[10]This follows from the assumption that volatilities of firms' liabilities are not significant, as can be seen from the mathematical relationship between volatilities of leverage ratio, firm's asset values and liabilities in Appendix A of Hui et al. (2006). Under this assumption the volatility of the leverage ratio is then close to the volatility of the firm asset value.

Credit Rating	AAA	AA	A	BBB	BB	B	CCC
Leverage ratios L_i (%)	3.1	9.5	17.2	31.5	49.5	53.8	73.2
Volatilities σ_i	0.127	0.156	0.184	0.213	0.241	0.270	0.299

TABLE 2. Parameters used for individual ratings.

values of which are close to the estimates of Delianedis & Geske (1999), who observed that the volatility value is 0.17 for AA and A-rated firms and 0.27 for B-rated firms. Taking these values as reference points, volatilities for other rating categories can be tabulated for each successive rated category. The values of leverage ratios and volatilities used for different individual ratings are shown in Table 2 which is reproduced from Table 1 of Hui et al. (2007).

The time horizon is fifteen years which is the same as in Hui et al. (2007), who compared the individual default probabilities to S&P historical cumulative default rates for which the available data is up to fifteen years.

We evaluate the joint survival probabilities based on the alternating direction implicit scheme outlined in Appendix I. The spatial steps used are $\Delta x = 8.47\text{E-}03$ and $\Delta y = 6.03\text{E-}03$ and the time step used is $\Delta t = 0.01$. The accuracy of this setting will be discussed in the following subsection and it is seen to result in a reasonable level of accuracy (error $< 1\%$ except at fifteen years where the error is around 1.3%).

The default correlations are evaluated based on the equation given in (24). The individual default probabilities are computed by using equation (17) for the case of constant coefficients and equation (22) for the case of time-varying coefficients. Note that all the valuations here are under the risk-neutral measure.

In the following subsections, we first investigate the accuracy of using different numerical methods; we then study the impact on joint survival probabilities and default correlations of a range of different scenarios, for example, paired firms having different credit quality, different values for correlation coefficients, drift levels, volatilities and initial leverage ratios, and the price of the credit linked note in subsection Subsection 4.8.

Douglas-Rachford ADI results compared to exact solutions				
Δt	Δx	Δy	$\rho_{12} = -0.9$	Relative % error
0.01	3.19E-02	2.27E-02	0.74884	0.15970%
0.01	8.47E-03	6.03E-03	0.74867	0.13714%
0.001	8.47E-03	6.03E-03	0.74779	0.01886%
0.001	4.21E-03	3.00E-03	0.74774	0.01321%
MOI exact results			0.74764	-

TABLE 3. Comparing of the joint survival probability based on ADI method to the exact solution MOI. The time period is one year and other parameters used are $L_1 = 73.2\%$, $L_2 = 31.5\%$, $\sigma_1 = 0.299$, $\sigma_2 = 0.213$, $\widetilde{\mu}_1 = \widetilde{\mu}_2 = 0$, $\rho_{1r} = \rho_{2r} = 0$, $\rho_{12} = -0.9$. These data are for a CCC-BBB rated pair of firms.

4.1. *Accuracy.*

When the coefficients are constant, the solution obtained by the method of images approach (in Subsection 3.3) is exact. Therefore, we use the method of images (MOI) results as a benchmark for comparing the accuracy of alternating direction implicit and the Monte Carlo method.

First, we compare alternating direction implicit results to the exact solution. We consider CCC-BBB paired firms. The exact analytical solution by the method of images is only valid for specific values of the correlation coefficient ρ_{12} (see Table 1), and we use $\rho_{12} = -0.9$ (corresponding to $\rho_{12} = -\cos\frac{\pi}{7}$ in Table 1). Note that x and y are volatility normalized log leverage ratios (i.e. $x = \ln(L_1/\widehat{L}_1)/\sigma_1$, $y = \ln(L_2/\widehat{L}_2)/\sigma_2$), thus in order to increase accuracy, spatial steps are chosen in a way that the given values of L_1 and L_2 are very close to grid points.

Table 3 shows that the relative percentage error of overall results are smaller than 1% for the time step is 0.01 and spatial steps less than 0.04. The result is further improved (error $< 0.02\%$) when the time step is 0.001 and spatial steps < 0.01. We have found that other choices of ρ_{12} (for example $\rho_{12} = 0$ and $\rho_{12} = -0.5$) give similar convergence results.

Next, we compare the Monte Carlo results to the exact solution in order to their accuracy. Table 4 shows that the relative percentage errors with $3,650$ time steps per year (i.e. 10 time steps in a day) is around 1% where the number of paths is $M = 500,000$ or $M = 1,000,000$. The relative percentage errors are reduced further to $< 0.4\%$ when the number of time steps is increased to $36,500$ (i.e. 100 time steps in a day).

Monte Carlo results compared to exact solutions			
n	M	$\rho_{12} = -0.9$	Relative % error
3,650	500,000	0.2835	1.1670%
3,650	1,000,000	0.2830	0.9590%
36,500	500,000	0.2812	0.3243%
36,500	1,000,000	0.2804	0.0549%
MOI exact results		0.2803	-

TABLE 4. Comparing of the joint survival probabilities based on the Monte Carlo method to the exact solution of MOI. The time period is fifteen years and other parameters used are $L_1 = 73.2\%$, $L_2 = 31.5\%$, $\sigma_1 = 0.299$, $\sigma_2 = 0.213$, $\widetilde{\mu}_1 = \widetilde{\mu}_2 = 0$, $\rho_{1r} = \rho_{2r} = 0$, $\rho_{12} = -0.9$. These data are for a CCC-BBB rated pair of firms.

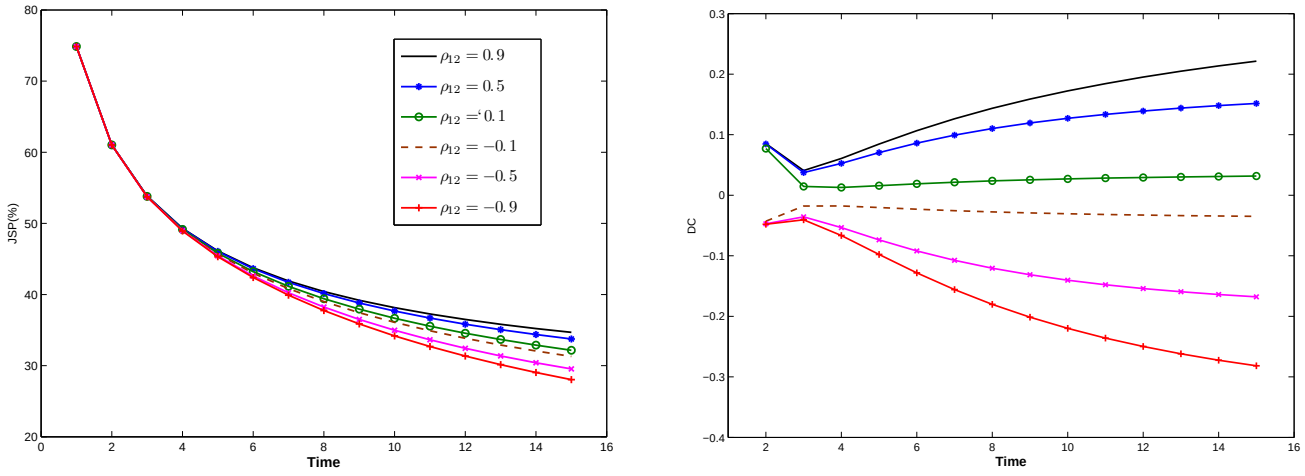

(a) JSP (b) DC

FIGURE 2. (a) shows the impact of the correlation coefficient ρ_{12} on joint survival probability; (b) shows the impact of the correlation coefficient ρ_{12} on default correlation. Here CCC-BBB paired firms are used and parameters used are L_1=73.2%, L_2=31.5%, σ_1=0.299, σ_2 =0.213, $\widetilde{\mu}_1 = \widetilde{\mu}_2 = 0$, $\rho_{1r} = \rho_{2r} = 0$, $\rho_{12} = -0.9, -0.5, -0.1, 0.5$ and 0.9.

We note that when coefficients are time-dependent, the solution obtained by the method of images approach is not exact (see Subsection 3.4). Therefore, we use the Monte Carlo results as a benchmark for comparing the accuracy of the the approximate solution of MOI results and the ADI results. Table 5 shows that the relative percentage error of the approximate results of the MOI over time is $< 1\%$. The relative percentage error of the ADI results overall are less than 1% except at fifteen years (around 1.3%).

4.2. *The Impact of Correlation Between Two Firms.*

Year	MC	MOI	Relative % error of MOI to MC	ADI	Relative % error of ADI to MC
1	0.7421	0.7409	-0.1587	0.7419	-0.0230
2	0.5997	0.5988	-0.1562	0.5994	-0.0567
3	0.5249	0.5240	-0.1612	0.5244	-0.0907
4	0.4766	0.4757	-0.1861	0.4760	-0.1330
5	0.4408	0.4405	-0.0652	0.4407	-0.0224
6	0.4134	0.4131	-0.0762	0.4132	-0.0399
7	0.3912	0.3907	-0.1167	0.3908	-0.0846
8	0.3725	0.3719	-0.1555	0.3721	-0.1260
9	0.3563	0.3559	-0.1318	0.3560	-0.1034
10	0.3424	0.3419	-0.1319	0.3420	-0.1016
11	0.3301	0.3297	-0.1411	0.3299	-0.1017
12	0.3193	0.3188	-0.1376	0.3191	-0.0696
13	0.3096	0.3092	-0.1103	0.3097	0.0403
14	0.3009	0.3008	-0.0101	0.3020	0.3698
15	0.2930	0.2939	0.3063	0.2969	1.3387

TABLE 5. The accuracy of MOI for time-dependent coefficients that was developed in Subsection 3.4, and the accuracy of the ADI method by comparing the results of joint survival probability to the MC results. The time period is fifteen years and other parameters used are $L_1 = 73.2\%$, $L_2 = 31.5\%$, $\sigma_1 = 0.299$, $\sigma_2 = 0.213$, $\widetilde{\mu}_1 = \widetilde{\mu}_2 = 0$, $\rho_{12} = -0.9$ and $\rho_{1r} = \rho_{2r} = -0.75$. For the MC method we use: $N_t = 36500$ and $M = 1$ million. For the ADI method we use: $\Delta\tau = 0.01$, $\Delta x = 8.47\text{E-}03$ and $\Delta y = 6.03\text{E-}03$.

We use the CCC and BBB paired firms to demonstrate the correlation effect. We consider the correlation levels of $\rho_{12} = -0.9, -0.5, -0.1, 0.5$ and 0.9. In order to isolate the effects of the drift terms of the leverage ratio processes and correlation of the interest rate process, we set $\widetilde{\mu}_i$=0 and ρ_{ir}=0 (i=1,2). We will study later in this section the impact of these two factors on joint survival probabilities and default correlations.

Figure 2-(a) plots the joint survival probability of firm i (i=1,2) from the beginning to the end of the investment period of fifteen years. It shows the impact on joint survival probabilities of the correlation coefficient ρ_{12} between CCC-BBB paired firms over the time horizon. First, we observe that the joint survival probability declines over time. Second, the joint survival probability decreases with the level of correlation coefficient ρ_{12}. It reflects the fact that when firms' leverage ratios move in the opposite direction there is a lower joint survival probability than when the move is in the same direction. When firms' leverage ratios move in opposite directions, as the leverage ratio of firm one moves closer to the default barrier (and so is more

unlikely to survive), the second firm moves away from the default barrier (and more likely to survive), so the chance of both firms surviving is small, because the two firms are always in opposite situations. While when firms' leverage ratios move in the same direction, for example both firms' leverage ratios moves away from the default barrier (and both firms more likely to survive at the same time). In case of firm's leverage ratios move closer to the default barrier at the same time, the default probability of both firms default at the same time increases, while the chance of default separately decreases. Recall (25), as a result the joint survival probability increases.

We also observe that the variation of ρ_{12} makes little difference to the value of the joint survival probabilities with there being no discernable difference up to six years and a difference of 6.71% at fifteen years for $\rho_{12} = 0.9$ and -0.9.

Figure 2-(b) plots the default correlation of firm one and the second firm from the beginning to the end of the investment period of fifteen years. The figure shows the impact on default correlations of the correlation coefficient ρ_{12} between CCC-BBB paired firms. First, we note that the sign of default correlations are the same as the correlation coefficient between two firms' leverage ratios ρ_{12}, which agrees with what was found by Zhou (2001) and Cathcart & El-Jahel (2002). Second, we observe that the magnitude of default correlation values (i.e. the absolute values) increase as the absolute values of correlation coefficient ρ_{12}. Here, the magnitude of default correlation measures the strength of default of firm one relative to the second firm, and the sign of default correlation indicates how this default signal works on the second firm.

In case of positive correlation coefficient, the second firm will be distressed as the default of firm one and is more likely to default at the same time. An example is that firm one is the creditor of the second firm, as firm one defaults, the second firm becomes distressed and is more likely to default at the same time. Consider the two-firm model here, if firms' leverage ratios are positively correlated, as firm one defaults, the default signal will cause the rise of second firm's leverage ratio and it will move closer to the default barrier, thus increasing the probability of second firm defaulting at the same time.

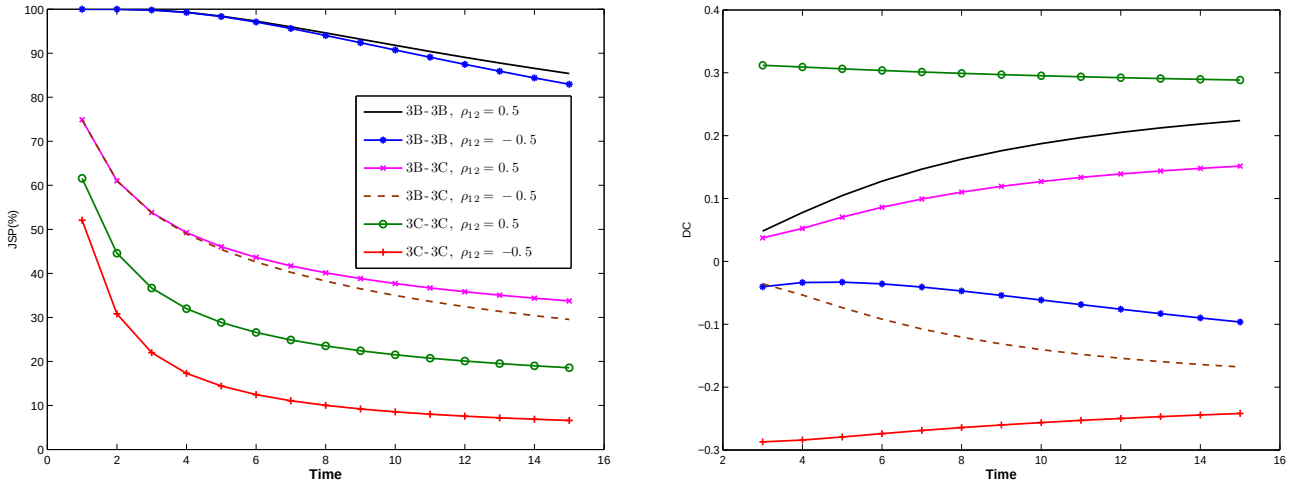

(a) JSP (b) DC

FIGURE 3. (a) shows the impact of different credit rated pairing of firms on joint survival probability; (b) shows the impact of different credit rated pairing of firms on default correlation. Here CCC-CCC, CCC-BBB and BBB-BBB paired firms are used and parameters used are L_{CCC}=73.2%, L_{BBB}=31.5%, σ_{CCC}=0.299, σ_{BBB} =0.213, $\widetilde{\mu}_1 = \widetilde{\mu}_2 = 0$, $\rho_{1r} = \rho_{2r} = 0$, $\rho_{12} = -0.5$ and 0.5.

In case of negative correlation coefficient, the second firm will benefit from the default of firm one. For example, if the two firms are competitors, then if firm one defaults, the second firm might profit by obtaining its customers and receiving a discount from its suppliers, as such, the second firm will be less likely to default at the same time. From the modelling point of view, if firms leverage ratios are negatively correlated, the default signal from firm one will cause the second firm's leverage ratio move in opposite direction and away from the default barrier, thus the second firm is less likely to default at the same time.

We also note that the default correlation values at the very beginning of the time horizon are rising. This is an artificial effect due to division by the very small values of individual default probability for BBB-rated firm (for example, $\mathrm{PD}_{\mathrm{BBB}} = 6.97838 \times 10^{-5}$). In order to avoid division by the extreme small values, in the remaining figures (part (b) only), the plot of default correlations will start at time equal to three years.

4.3. *The Impact of Different Credit Quality Paired Firms.*

This subsection shows the impact of the difference of the credit pairing of firms on joint survival probabilities and default correlations by using CCC-CCC, CCC-BBB and BBB-BBB pairing

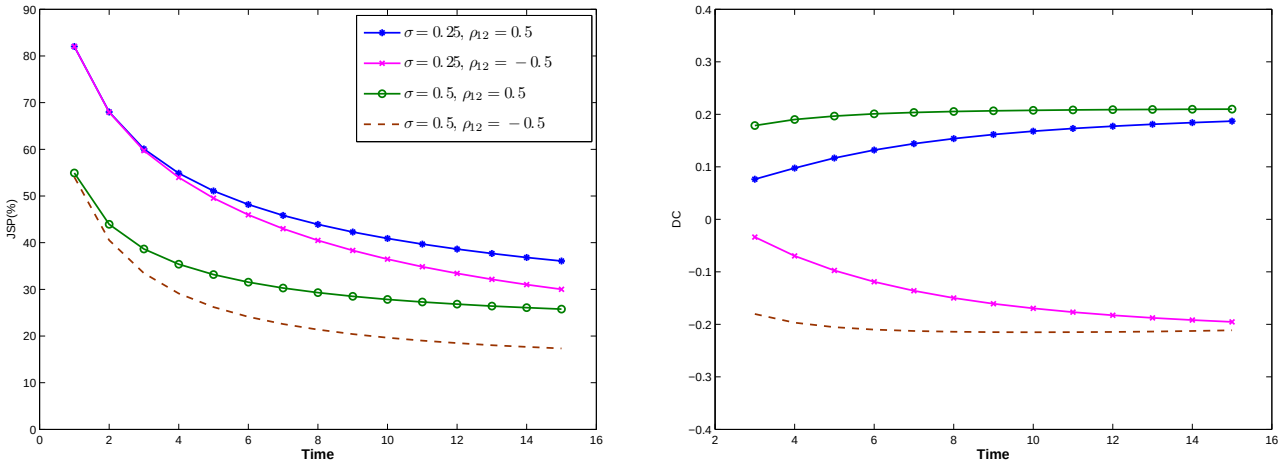

(a) JSP (b) DC

FIGURE 4. (a) shows the impact of volatility levels on joint survival probability; (b) shows the impact of volatility levels on default correlation. Here CCC-BBB paired firms are used and parameters used are $L_1 = 73.2\%$, $L_2 = 31.5\%$, $\sigma_1 = \sigma_2 = \sigma = 0.25$ and 0.5, $\widetilde{\mu}_1 = \widetilde{\mu}_2 = 0$, $\rho_{1r} = \rho_{2r} = 0$, $\rho_{12} = -0.5$ and 0.5.

of firms. To illustrate the effect of positive and negative correlation between two firms, the two non-extreme values of correlation coefficient $\rho_{12} = -0.5, 0.5$ are used here and in the rest of the section.

Figure 3-(a) shows the impact on joint survival probabilities for CCC-CCC, CCC-BBB and BBB-BBB pairing of firms. First, we observe that the JSP of good credit quality firms is higher than that of low credit quality firms. Second, we find that JSP curves decrease slowly over time for BBB-BBB paired firms, while for CCC-CCC paired firms, JSP curves quickly in the short term and flatten out towards long run. We also notice that the effect of leverage ratio correlation on CCC-CCC paired firm is more significant than BBB-BBB paired firm, where lower credit quality firms are more sensitive to the change of correlation levels than that of good credit quality firms.

For good credit quality firms, their initial leverage ratios are lower and distant from the default barrier, therefore, the joint survival probability is higher than for lower credit quality firms. If firm one has defaulted, the second firm will experience a rise (decline) in its leverage ratio because of the positive (negative) correlation, however, because of the low initial leverage ratio of the second firm, this rise (decline) in the leverage ratio of the second firm does not effect significantly its default probability. However, if the second firm is of low credit quality, its initial

leverage ratio is high and closer to the default barrier, this rise (decline) in leverage ratios will increase the probability of bringing the second firm into default.

Figure 3-(b) illustrates the impact on default correlations. It shows that at a given maturity the absolute values of DC increases as the firm's credit quality decreases. It shows the fact that the lower is the credit quality of paired firms, the higher the strength of default of firm one relative to the second firm. However, an interesting result is that for a good quality (BBB-BBB) pair of firms, if they are positively correlated, the default correlation is higher than that of a good quality and low quality pairing of firms. But this situation is reversed (as far as the comparison of the absolute values of default correlation is concerned) if they are negatively correlated. It is difficult to relate this finding to any empirical evidence, though clearly it points to the need for more empirical research in this area. We also observed that DC curves of CCC-CCC increase quickly at the short term and flatten at the long-term, however DC curves of BBB-BBB and CCC-BBB paired firms increase slowly over time. These effects make sense in that the impact of firm one defaulting on the second firm occurs quickly for low credit quality firms, but for good credit quality firms, such an impact increases gradually over time.

4.4. *The Impact of Volatilities.*

We consider the volatility levels ranging between $\sigma_i = 0.25$ and 0.5. Figure 4-(a) shows that the higher the volatility level the lower the joint survival probability. This result seems reflect the fact that when the proportional change in leverage ratios is more volatile, the chance of the leverage ratio hitting the default point is higher, so the joint survival probability is lower.

Figure 4-(b) shows that the values of default correlation increase with volatility levels. In terms of the two-firm model, the higher the volatility level, the larger the range in which the leverage ratio can move. For example, when firm one defaults, the impact on the second firm's leverage ratio can move with a larger amplitude towards the default barrier (if firms are positively correlated) than the smaller amplitude when using a smaller volatility level, therefore the probability of the second firm defaulting at the same time increases. We also note that the effect of changing volatility level on DC is more significant at the short term.

4.5. *The Impact of Drift Levels.*

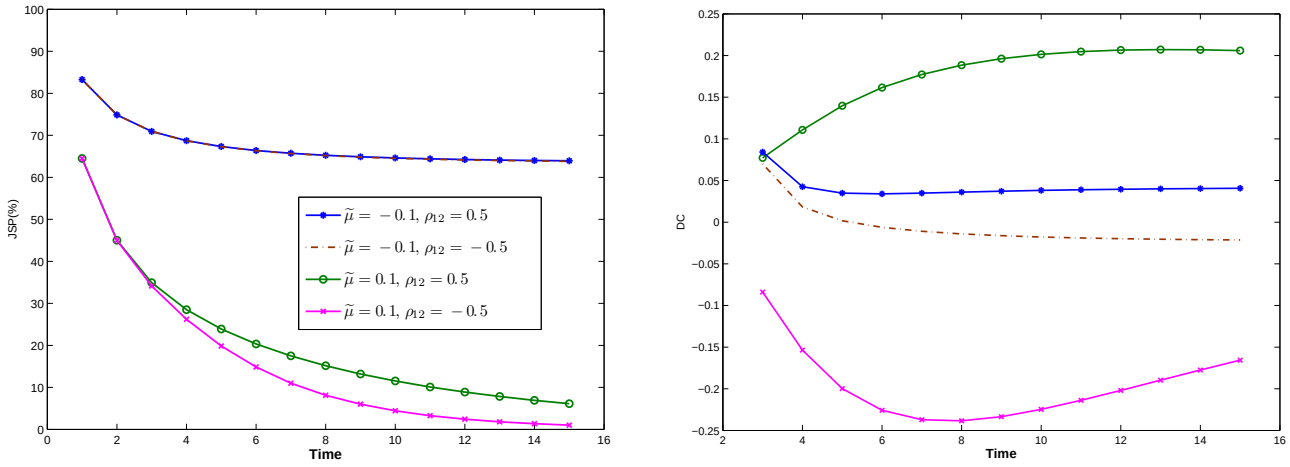

(a) JSP (b) DC

FIGURE 5. (a) shows the impact of mean levels on joint survival probability; (b) shows the impact of mean levels on default correlation. Here CCC-BBB paired firms are used and parameters used are L_1=73.2%, L_2=31.5%, σ_1=0.299, σ_2 =0.213, $\widetilde{\mu}_1 = \widetilde{\mu}_2 = \widetilde{\mu} = -0.1$ and 0.1, $\rho_{1r} = \rho_{2r} = 0$, $\rho_{12} = -0.5$ and 0.5.

We consider the drift levels $\widetilde{\mu}_1 = \widetilde{\mu}_2 = -0.1, 0, 0.1$. Note that $\widetilde{\mu}_i$ is under the risk-neutral measure. Figure 5-(a) shows that the joint survival probability increases as the drift level decreases. Recall that it is the growth rate of proportional changes in the leverage ratio, which means the higher the drift level, the higher the leverage ratio over time, and thus the probability of leverage ratio hitting the default barrier is high, therefore the joint survival probability declines with the rise of the drift level. We note that the joint survival probability is very sensitive to the change of drift levels. We also observe that the effect of the correlation coefficient ρ_{12} is more pronounced for larger values of drift levels. There is no significant impact of ρ_{12} on joint survival probabilities in the case of negative drift, but a noticeable impact when the value of the drift is positive. For example, if the drift is negative, then this would mean a negative growth rate of the proportional change in leverage ratio on average, where a firm's leverage ratio decreases and moves away from the default barrier over time. If firm one defaults, the second firm will be less impacted because its leverage ratio is heading away from the default barrier even though the correlation coefficient is positive (note that the impact of ρ_{12} is no significant for negative drift), and so is less likely to default at the same time. The situation will reverse itself for a positive drift.

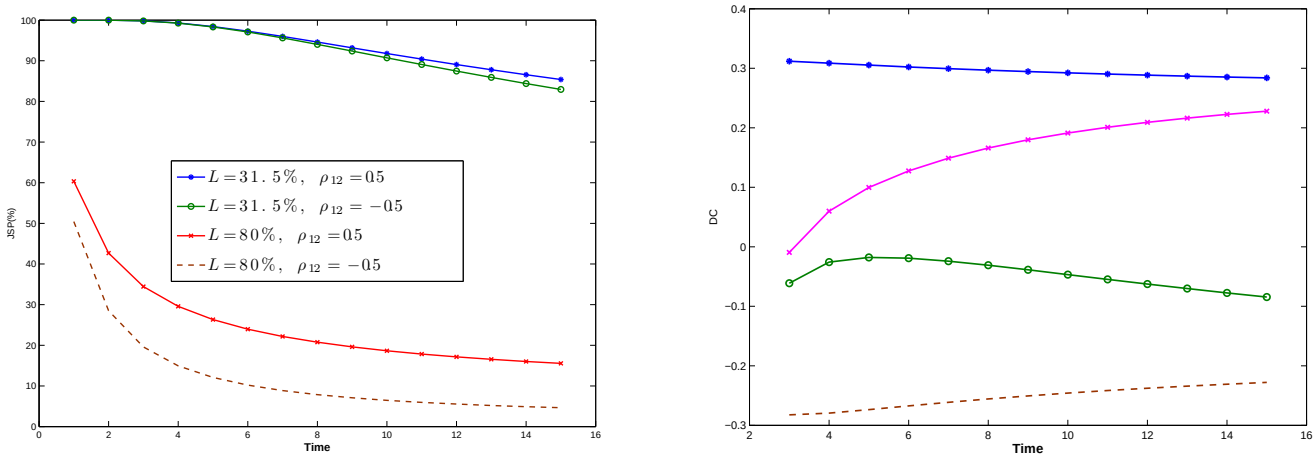

(a) JSP (b) DC

FIGURE 6. (a) shows the impact of leverage ratio levels on joint survival probability; (b) shows the impact of leverage ratio levels on default correlation. Here initial leverage ratios used in case (i) are $L_1 = L_2 = L = 31.5\%$ and in case (ii) are $L_1 = L_2 = L = 80\%$. Other parameters used are $\sigma_1 = \sigma_2 = 0.213$, $\widetilde{\mu}_1 = \widetilde{\mu}_2 = 0$, $\rho_{1r} = \rho_{2r} = 0$, $\rho_{12} = -0.5$ and 0.5.

Figure 5-(b) shows that the default correlation is sensitive to the change in the drift levels. It also shows that the higher the drift level, the higher values of default correlation. If a firm's leverage ratio grows to a higher value on average, the credit quality of the firm decreases dramatically, and the impact on default correlation is similar to the previous discussion (see Subsection 4.3) on the impact of different credit quality firms, that is the lower the credit quality of firms, the higher the strength of default of firm one relative to the second firm.

4.6. *The Impact of Initial Value of Leverage Ratio Levels.*

We consider the initial value of leverage ratio levels $L_1 = L_2 = 31.5\%$ (corresponding to BBB-rated firms) and $L_1 = L_2 = 80\%$ (corresponding to CCC-rated firms). Figure 6-(a) shows the joint survival probability generally decreases over time. It shows that the lower the initial value of leverage ratio levels, the higher the joint survival probability. The joint survival probability is more sensitive to the change in the correlation coefficient ρ_{12} when the initial value of leverage ratio is high. This result is similar to the results observed in Figure 3-(a). Figure 6-(b) shows that the higher the leverage ratio levels, the higher the default correlations (in absolute values). That is the lower the quality of these two firms, the grater is the default probability between them.

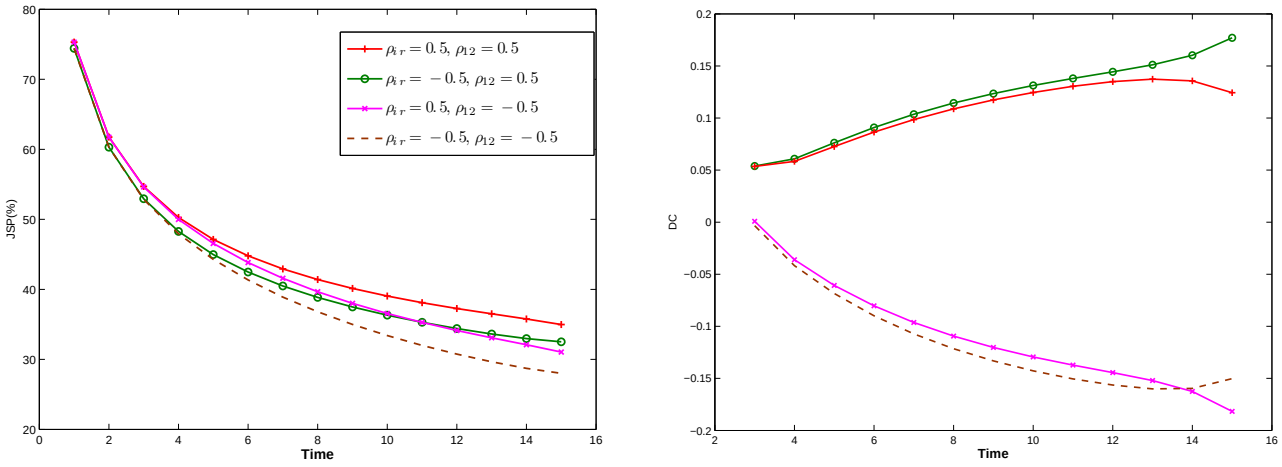

(a) JSP (b) DC

FIGURE 7. (a) shows the impact of the correlation coefficient ρ_{ir} on joint survival probability; (b) shows the impact of the correlation coefficient ρ_{ir} on default correlation. Here CCC-BBB paired firms are used and parameters used are $L_1 = 73.2\%$, $L_2 = 31.5\%$, $\sigma_1 = 0.299$, $\sigma_2 = 0.213$, $\widetilde{\mu}_1 = \widetilde{\mu}_2 = 0$, $\rho_{12} = -0.5, 0.5$, $\rho_{1r} = \rho_{2r} = -0.5, 0.5$, the maturity of risk-free bond price is $T = 15$, $\kappa_r = 1.0$ and $\sigma_r = 0.03162$.

4.7. *Impact of Correlation Between Firms & Interest Rates.*

This subsection presents the impact of interest rate risk on joint survival probabilities and default correlations. Note that when the correlation to the interest ratio process ρ_{ir} is non-zero, the joint survival probability and the probability of individual defaults are related to the parameter κ_r that controls the speed of the mean reversion of the interest rate process via the time-dependent coefficient $b(t)$, which is given in (41). We consider $\kappa_r = 1.0$, $\sigma_r = 0.03162$ which is consistent with the values used by Hui et al. (2007). The values of the correlation coefficients between firms' leverage ratios and interest rates are take the mid values $\rho_{1r} = \rho_{2r} = -0.5, 0.5$.

Figure 7-(a) shows that the joint survival probability increases as the correlation coefficient ρ_{ir} increases. Recall (41), which is a negative time-dependent function, thus the drift of the leverage ratio is actually proportional negatively to the correlation level. Therefore, the higher the correlation coefficient ρ_{ir}, the smaller the drift level, and so the leverage ratio moves to a smaller value on average. At a lower leverage ratio level, the chance of hitting the default barrier is smaller, and thus the higher the chance of surviving over time. But we note that the effect of the interest rate becomes weaker at about year 13 where the the solid line with crosses and solid line with circles cross. This effect comes from the time-dependent function $b(t)$, and

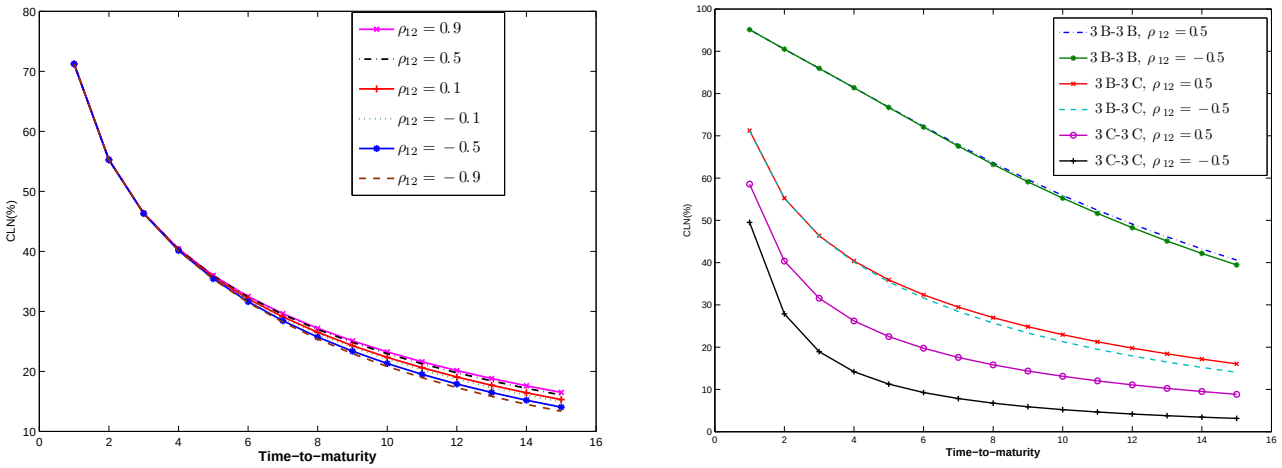

(a) CLN (b) CLN

FIGURE 8. (a) shows the impact of the correlation coefficient ρ_{12} on credit linked note prices, where CCC-BBB paired firms are used; (b) shows the impact of different credit rated pairing of firms credit linked note prices, where CCC-CCC, CCC-BBB and BBB-BBB paired firms are used. Here parameters used are L_{CCC}=73.2%, L_{BBB}=31.5%, σ_{CCC}=0.299, σ_{BBB} =0.213, $r = 5\%$, $\kappa_r = 1$, $\widetilde{\theta}_r = 5\%$, $\sigma_r^2 = 0.001$, $\widetilde{\mu}_1 = \widetilde{\mu}_2 = 0$, $\rho_{1r} = \rho_{2r} = 0$ and the payoff is 1. The correlation coefficient ρ_{12} used in (a) is $\rho_{12} = -0.9, -0.5, -0.1, 0.5$ and 0.9; in (b) is $\rho_{12} = -0.5$ and 0.5.

thus the interest rate impact on the drift rate is time varying. We also observe that the joint survival probability is not very sensitive to the change of the correlation level to interest rate risk.

Figure 7-(b) shows that the level of DC increases as the correlation coefficient ρ_{ir} declines, but the impact is not significant. We also observe the time varying function of interest rate parameters impact on the DC at about year 13, which is similar to the result of observed in Figure 7-(a).

4.8. *The Price of Credit Linked Notes.*

The focus of this paper has mostly been on default correlations and joint survival probabilities, but the other application of the two-firm model is to price the credit linked note. In this subsection, we illustrate the impact on the prices of credit linked notes with respect to variation in the values of correlation coefficients between two firms and with respect to different credit quality paired firms.

Recall from (36) that the price of a credit linked note is the product of the function $\widehat{P}(L_1, L_2, t)$ and the risk-free bond price $B(r, t)$ of the Vasicek (1977) model[11]. For the numerical calculations we use parameters similar to Hui et al. (2007), where $r = 5\%$, $\kappa_r = 1$, $\widetilde{\theta}_r = 5\%$ and $\sigma_r^2 = 0.001$.

Figure 8-(a) shows the impact on credit linked note prices of different values of the correlation coefficient ρ_{12} of a BBB-CCC paired firms. The parameters used to calculate $\widehat{P}(L_1, L_2, t)$ are the same as in Figure 2-(a). We observe that the credit linked note prices decrease with respect to time-to-maturity as the correlation coefficient ρ_{12} decreases. This may be due to the fact that when firms' leverage ratios move in the same direction the price of a credit linked note is higher than that for moves in the opposite direction. If firms' leverage ratios move in opposite directions, as one firm's leverage ratio moves closer to the default barrier (and is less likely to survive), the second firm moves away from the default barrier (and is more likely to survive), so the chance of both firms surviving is small because they are always moving in opposite directions, therefore, the price of credit linked note is lower.

Figure 8-(b) shows the impact on credit linked note prices for BBB-BBB, BBB-CCC and CCC-CCC paired firms over the time-to-maturity. The parameter used to evaluate $\widehat{P}(L_1, L_2, t)$ are the same as in Figure 3-(a). We observe that the price of a credit linked note of BBB-BBB paired firms is the highest, while the price of CCC-CCC paired firms is the lowest. This result seems sensible since the price of credit linked note issued by good credit quality firms is higher than that issued by lower credit quality firms.

We also observe that the impact of the correlation coefficient ρ_{12} or the credit quality of firms on the price of credit linked note is the same as the impact on joint survival probabilities (see Figure 2-(a) and Figure 3-(a)). This is because the function (48) and the joint survival probability function (57) both depend principally on the same transition probability density function, as the payoff of the credit linked note is the par value (see (31)). Therefore, if we use the same risk-free bond price function, the impact of other parameters on credit linked note prices will be similar to the impact on joint survival probabilities as illustrated in previous subsections.

[11]The solution of the Vasicek model can be found for example in Wilmott, Howison & Dewynne (1995) or Hull (2000).

5. Conclusion

The aim of this article has been to extend the dynamic leverage ratio model for Hui et al. (2007) to the two-firm case so as to study its implications for default correlations and joint survival probabilities.

In Section 2, we reviewed the one-firm dynamic leverage ratio model of Hui et al. (2007) for corporate bond pricing. In their model, by using of the method of separation of variables, the corporate bond price can be interpreted as the product of a riskless bond price and a function depending only on the firm's leverage ratio. The risk-free bond price has a known closed-form solution, therefore the main focus is on solving for the partial differential equation that depends only on the firm's leverage ratio. We reviewed the method of images approach for obtaining a closed-form solution in terms of cumulative normal distribution functions and then the time varying barrier method proposed by Lo et al. (2003) to deal with the case in which parameters are time varying.

In Section 3, we developed the framework for the dynamic leverage ratio model in the two-firm situation for pricing financial derivatives involving default risks among two firms using the credit linked note as the motivating example. We showed that the problem can be reduced to that of solving the partial differential equation for a function depends only on the two firms' leverage ratios. We also extended the method of images approach to the two-dimensional heat equation case and obtained the analytical solution subject to zero boundary conditions. This result was then applied to solve the partial differential equation for the function with constant coefficients. For coefficients in the time-dependent case, we extended the time varying barrier approach to obtain an approximate solution. However, we saw that the limitation of the method of images approach applied in the two-dimensional situation is that it works only for certain values of the correlation coefficient between the dynamic leverage ratios of firms.

In order to obtain solutions for general values of the correlation coefficient, we considered the alternating direction implicit numerical method in Subsection 3.5, developing in particular the alternating direction implicit numerical scheme based on Douglas & Rachford (1956). We also

developed a Monte Carlo scheme to serve as a benchmark. A discussion on the accuracy for different methods is shown in Subsection 4.1.

In Section 4, we investigated the impact on joint survival probabilities and default correlations of different values of the model parameters. The main finding were that the joint survival probabilities rise if there is (i) a decrease in the leverage ratio volatility, the average mean levels, the initial leverage ratios, or (ii) an increase in the correlation coefficient between leverage ratios processes, or in the correlation coefficient between leverage ratio and interest rate processes. We also found that the default correlation (in absolute values) rises if there is (i) an increase in the firms' leverage ratios correlation, or their volatilities, or average mean levels, or initial leverage ratios, or (ii) a decrease in the correlation between firm's leverage ratio and the interest rate.

We note that these findings are based on a study of the impact of the model parameters chosen. Whilst there is a rationale for these values as we have explained, it remains a task for future research to calibrate the types of model discussed here to market data.

Appendix A. The Method of Images and the Derivation of Equation (15)

Consider the heat equation

$$\frac{\partial u}{\partial \tau} = \frac{1}{2}\frac{\partial^2 u}{\partial x^2}, \tag{A-1}$$

where x is unrestricted in the region $x \in (-\infty, \infty)$. The solution to (A-1) is known[12] to be of the form

$$u(x,\tau) = \int_{-\infty}^{\infty} g(x,y;\tau)u(y)dy, \tag{A-2}$$

where $u(y)$ is the initial condition function, g is the transition probability density function that has the form

$$g(x,y;\tau) = \frac{e^{-(x-y)^2/2\tau}}{\sqrt{2\pi\tau}}. \tag{A-3}$$

[12]The solution of the heat equation can be found in many reference. For example, Wilmott et al. (1995) (Chpaters 4 and 5) give a good discussion and derivation of the solution of the heat equation.

If a zero boundary condition is imposed along x-axis at $x = 0$, then

$$u(0, \tau) = 0, \tag{A-4}$$

and the region of interest for the solution becomes $x \in (-\infty, 0)$. Applying the method of images approach, the exact solution to the heat equation (A-1) subject to the zero boundary condition (A-4) is

$$u(x, \tau) = \int_{-\infty}^{0} \widetilde{g}(x, y; \tau) u(y) dy, \tag{A-5}$$

where $\widetilde{g}$ is the transition probability density function for the restricted process. It is obtained by subtracting from the original density g (for the unrestricted process) centered at y within the ("physical") region $y \in (-\infty, 0)$ the same density centered at $-y$ within the ("nonphysical") region $y \in (0, \infty)$, that is

$$\widetilde{g}(x, y; \tau) = g(x, y; \tau) - g(x, -y; \tau), \tag{A-6}$$

so that the the boundary condition (A-4) is satisfied, as is easily verified.

Next, consider the case in which the coefficients in (10) are constant, that is $\sigma_L(\tau) = \sigma_L$ and $\gamma(\tau) = \gamma$, and the partial differential equation becomes

$$\frac{\partial \bar{P}}{\partial \tau} = \frac{1}{2}\sigma_L^2 \frac{\partial^2 \bar{P}}{\partial x^2} + \gamma \frac{\partial \bar{P}}{\partial x}. \tag{A-7}$$

The partial differential equation (A-7) can be reduced to the heat equation (A-1).

Proposition 1. *The solution to the partial differential equation (A-7) may be written*

$$\bar{P}(x, \tau) \;\; = \;\; e^{\eta x + \xi \tau} u(x, \zeta), \tag{A-8}$$

where η, ξ and ζ are constants given by

$$\eta = -\frac{\gamma}{\sigma_L^2}, \;\; \xi = -\frac{\gamma^2}{2\sigma_L^2}, \;\; \zeta = \sigma_L^2 \tau,$$

and $u(x,\zeta)$ satisfies the partial differential equation

$$\frac{\partial u}{\partial \zeta} = \frac{1}{2}\frac{\partial^2 u}{\partial x^2}. \tag{A-9}$$

Proof: Calculate

$$\frac{\partial \bar{P}}{\partial \tau} = e^{\eta x+\xi\tau}\left[\xi u + \frac{\partial u}{\partial \tau}\right],\ \frac{\partial \bar{P}}{\partial x} = e^{\eta x+\xi\tau}\left[\eta u + \frac{\partial u}{\partial x}\right],\ \frac{\partial^2 \bar{P}}{\partial x^2} = e^{\eta x+\xi\tau}\left[\eta^2 u + 2\eta\frac{\partial u}{\partial x} + \frac{\partial^2 u}{\partial x^2}\right]. \tag{A-10}$$

Substituting from equations (A-10) into equation (A-7), the partial differential equation reduces to

$$\begin{aligned}\frac{\partial u}{\partial \tau} &= \frac{1}{2}\sigma_L^2\left[\eta^2 u + 2\eta\frac{\partial u}{\partial x} + \frac{\partial^2 u}{\partial x^2}\right] + \gamma\left[\eta u + \frac{\partial u}{\partial x}\right], \\ &= \frac{1}{2}\sigma_L^2\frac{\partial^2 u}{\partial x^2} + (\sigma_L^2\eta + \gamma)\frac{\partial u}{\partial x} + (-\xi + \frac{1}{2}\sigma_L^2\eta^2 + \gamma\eta)u. \end{aligned} \tag{A-11}$$

The $\frac{\partial u}{\partial x}$ and u terms can be eliminated by choosing

$$\sigma_L^2\eta + \gamma = 0 \quad \Rightarrow \quad \eta = -\frac{\gamma}{\sigma_L^2}, \tag{A-12}$$

$$-\xi + \frac{1}{2}\sigma_L^2\eta^2 + \gamma\eta = 0 \quad \Rightarrow \quad \xi = -\frac{1}{2}\frac{\gamma^2}{\sigma_L^2}, \tag{A-13}$$

the (A-11) becomes

$$\frac{\partial u}{\partial \tau} = \frac{1}{2}\sigma_L^2\frac{\partial^2 u}{\partial x^2}. \tag{A-14}$$

Since $u(x,\zeta)$ depends on ζ, we can express $\frac{\partial u}{\partial \tau} = \frac{\partial \zeta}{\partial \tau}\frac{\partial u}{\partial \zeta}$, then (B-20) becomes

$$[\sigma_L^2]^{-1}\frac{\partial \zeta}{\partial \tau}\frac{\partial u}{\partial \zeta} = \frac{1}{2}\frac{\partial^2 u}{\partial x^2}, \tag{A-15}$$

In order to eliminate the term $[\sigma_L^2]^{-1}$, we choose ζ to satisfy

$$[\sigma_L^2]^{-1}\frac{\partial \zeta}{\partial \tau} = 1, \tag{A-16}$$

from which

$$\zeta \;=\; \sigma_L^2 \tau. \tag{A-17}$$

So that (A-15) reduces to the heat equation (A-9).

■

The initial conditions for the function $\bar{P}$ and the heat equation u are related by $\big($setting $\bar{P}(y,0) = \bar{P}(y)$ and $u(y,0) = u(y)\big)$

$$\bar{P}(y) = 1 = e^{\eta y} u(y), \tag{A-18}$$

so that

$$u(y) = e^{-\eta y}. \tag{A-19}$$

Substituting the relations (A-8) and (A-19) into (A-5), yields

$$e^{-\eta x - \xi \tau} \bar{P}(x,\tau) = \int_{-\infty}^{0} \widetilde{g}(x,y;\zeta) e^{-\eta y} \bar{P}(y) dy. \tag{A-20}$$

Rearranging equation (A-20), the solution (15) is obtained.

Appendix B. The Derivation of Equation (21)

Consider a transformation of the partial differential equation

$$\frac{\partial \bar{P}_\beta}{\partial \tau} = \frac{1}{2}\sigma_L^2(\tau) \frac{\partial^2 \bar{P}_\beta}{\partial x^2} + \gamma(\tau) \frac{\partial \bar{P}_\beta}{\partial x}, \tag{B-1}$$

by setting

$$\bar{P}_\beta(x,\tau) = e^{-x^*(\tau)\frac{\partial}{\partial x}} \widetilde{P}(x,\zeta), \tag{B-2}$$

where $\zeta = \int_0^\tau \sigma_L^2(v) dv$ and the function $\widetilde{P}(x,\zeta)$ satisfies

$$\frac{\partial \widetilde{P}}{\partial \zeta} \;=\; \frac{1}{2}\frac{\partial^2 \widetilde{P}}{\partial x^2} - \beta \frac{\partial \widetilde{P}}{\partial x}. \tag{B-3}$$

$e^{\frac{\partial}{\partial x}}$ is an operator, it operates on an arbitrary, infinitely differentiable, function $f(x)$ according to

$$e^{c(\tau)\frac{\partial}{\partial x}} f(x) \;=\; \sum_{n=0}^{\infty} \frac{1}{n!} (c(\tau))^n \frac{\partial^n f(x)}{\partial x^n}, \tag{B-4}$$

where $c(\tau)$ is a time-dependent function.

A calculus for this operator has been developed in quantum mechanics for solving Fokker-Planck equations and Schrödinger equations, and is expounded for example in Suzuki (1989). Many of the results obtained using this operator calculus can be obtained by other approaches, however this calculus provides a convenient unified approach, for which we use it in this article.

To transform (B-1) to (B-3), we calculate

$$\frac{\partial}{\partial \tau} \big[e^{c(\tau)\frac{\partial}{\partial x}} f(x,\tau) \big], \tag{B-5}$$

by applying the Baker-Campbell-Hausdorff formula. The Baker-Campbell-Hausdorff formula is widely used in quantum mechanics to obtain a solution with combined exponentials of operators when these operators do not commute. The Baker-Campbell-Hausdorff formula is defined as (see for example, Hassani (1998), Chapter 2.2)

$$e^{\mathbf{A}} \mathbf{B} e^{-\mathbf{A}} \equiv \mathbf{B} + [\mathbf{A}, \mathbf{B}] + \frac{1}{2!}[\mathbf{A}, [\mathbf{A}, \mathbf{B}]] + \cdots, \tag{B-6}$$

where $\mathbf{A}$ and $\mathbf{B}$ are operators. The expression $[\mathbf{A}, \mathbf{B}]$ is called the commutator of two operators, and is defined as $[\mathbf{A}, \mathbf{B}] \equiv \mathbf{AB} - \mathbf{BA}$.

To carry out the operation in (B-5), we consider the following proposition.

Proposition 2. *The expression* (B-5) *may be written*

$$e^{c(\tau)\frac{\partial}{\partial x}} \Big[\frac{\partial f(x,\tau)}{\partial \tau} + \frac{\partial c(\tau)}{\partial \tau} \frac{\partial f(x,\tau)}{\partial x} \Big]. \tag{B-7}$$

Proof: First, we multiply (B-5) by the term

$$e^{c(\tau)\frac{\partial}{\partial x}} e^{-c(\tau)\frac{\partial}{\partial x}} \equiv 1, \tag{B-8}$$

to obtain

$$\left(e^{c(\tau)\frac{\partial}{\partial x}}e^{-c(\tau)\frac{\partial}{\partial x}}\right)\frac{\partial}{\partial \tau}\left[e^{c(\tau)\frac{\partial}{\partial x}}f(x,\tau)\right] = e^{c(\tau)\frac{\partial}{\partial x}}\left(e^{-c(\tau)\frac{\partial}{\partial x}}\frac{\partial}{\partial \tau}e^{c(\tau)\frac{\partial}{\partial x}}\right)f(x,\tau). \tag{B-9}$$

Considering the term in the bracket and applying the Baker-Campbell-Hausdorff formula (B-6) (setting $\mathbf{A} \equiv -c(\tau)\frac{\partial}{\partial x}$ and $\mathbf{B} \equiv \frac{\partial}{\partial \tau}$), we have

$$\begin{aligned}
&\left(e^{-c(\tau)\frac{\partial}{\partial x}}\frac{\partial}{\partial \tau}e^{c(\tau)\frac{\partial}{\partial x}}\right) \\
&= \frac{\partial}{\partial \tau} + [-c(\tau)\frac{\partial}{\partial x}, \frac{\partial}{\partial \tau}] + \frac{1}{2!}[-c(\tau)\frac{\partial}{\partial x}, [-c(\tau)\frac{\partial}{\partial x}, \frac{\partial}{\partial \tau}]] + \cdots, \\
&= \frac{\partial}{\partial \tau} + \left(-c(\tau)\frac{\partial}{\partial x}\cdot\frac{\partial}{\partial \tau} - \frac{\partial}{\partial \tau}\cdot(-c(\tau)\frac{\partial}{\partial x})\right) + 0, \\
&= \frac{\partial}{\partial \tau} + \frac{\partial c(\tau)}{\partial \tau}\frac{\partial}{\partial x}.
\end{aligned} \tag{B-10}$$

Note that the higher order terms vanish, as is quite straight forward to see, for example, by calculating the second term

$$\begin{aligned}
\frac{1}{2!}[-c(\tau)\frac{\partial}{\partial x}, [-c(\tau)\frac{\partial}{\partial x}, \frac{\partial}{\partial \tau}]] &= \frac{1}{2!}[-c(\tau)\frac{\partial}{\partial x}, \frac{\partial c(\tau)}{\partial \tau}\frac{\partial}{\partial x}] \\
&= -c(\tau)\frac{\partial}{\partial x}\cdot\frac{\partial c(\tau)}{\partial \tau}\frac{\partial}{\partial x} - \frac{\partial c(\tau)}{\partial \tau}\frac{\partial}{\partial x}\cdot(-c(\tau)\frac{\partial}{\partial x}) \\
&= -c(\tau)\frac{\partial c(\tau)}{\partial \tau}\frac{\partial^2}{\partial x^2} + c(\tau)\frac{\partial c(\tau)}{\partial \tau}\frac{\partial^2}{\partial x^2} = 0.
\end{aligned} \tag{B-11}$$

Substituting (B-10) into (B-9), we obtain

$$\frac{\partial}{\partial \tau}\left[e^{c(\tau)\frac{\partial}{\partial x}}f(x,\tau)\right] = e^{c(\tau)\frac{\partial}{\partial x}}\left[\frac{\partial f(x,\tau)}{\partial \tau} + \frac{\partial c(\tau)}{\partial \tau}\frac{\partial f(x,\tau)}{\partial x}\right]. \tag{B-12}$$

■

Apply the same approach, we have

$$\frac{\partial}{\partial x}\left[e^{c(\tau)\frac{\partial}{\partial x}}f(x,\tau)\right] = e^{c(\tau)\frac{\partial}{\partial x}}\left[\frac{\partial f(x,\tau)}{\partial x}\right], \tag{B-13}$$

and

$$\frac{\partial^2}{\partial x^2}\left[e^{c(\tau)\frac{\partial}{\partial x}}f(x,\tau)\right] = e^{c(\tau)\frac{\partial}{\partial x}}\left[\frac{\partial^2 f(x,\tau)}{\partial x^2}\right]. \tag{B-14}$$

Applying the relationship (B-12)-(B-14) to (B-2), we obtain

$$\frac{\partial \widetilde{P}}{\partial \tau} + \frac{\partial[-x^*(\tau)]}{\partial \tau}\frac{\partial \widetilde{P}}{\partial x} = \frac{1}{2}\sigma_L^2(\tau)\frac{\partial^2 \widetilde{P}}{\partial x^2} + \gamma(\tau)\frac{\partial \widetilde{P}}{\partial x}. \tag{B-15}$$

Note that if the dynamic form of $x^*(\tau)$ follows (19), we have $\frac{\partial[-x^*(\tau)]}{\partial \tau} = \gamma(\tau) + \beta\sigma_L^2(\tau)$, hence

$$\frac{\partial \widetilde{P}}{\partial \tau} = \frac{1}{2}\sigma_L^2(\tau)\frac{\partial^2 \widetilde{P}}{\partial x^2} - \beta\sigma_L^2(\tau)\frac{\partial \widetilde{P}}{\partial x}. \tag{B-16}$$

Define a new time-to-maturity variable

$$\zeta = \int_0^\tau \sigma_L^2(v)dv. \tag{B-17}$$

then $\widetilde{P}(x,\zeta)$ satisfies

$$\left[\sigma_L^2(\tau)\right]^{-1}\frac{\partial}{\partial \zeta}\left[\widetilde{P}\right]\frac{\partial \zeta}{\partial \tau} = \frac{1}{2}\frac{\partial^2 \widetilde{P}}{\partial x^2} - \beta\frac{\partial \widetilde{P}}{\partial x}. \tag{B-18}$$

As $[\sigma_L^2(\tau)]^{-1} \times \frac{\partial \zeta}{\partial \tau} = 1$, we obtained (B-3).

Note that the equation (B-3) has the constant coefficient only, we can apply the transformation described in Appendix A, by setting

$$\widetilde{P}(x,\zeta) = e^{\beta x - \beta^2\zeta/2}u(x,\zeta), \tag{B-19}$$

where $u(x,\zeta)$ satisfies the heat equation

$$\frac{\partial u}{\partial \zeta} = \frac{1}{2}\frac{\partial^2 u}{\partial x^2}. \tag{B-20}$$

Therefore, combine (B-2) and (B-19), we have

$$\bar{P}_\beta(x,\tau) = e^{-x^*(\tau)\frac{\partial}{\partial x}}\left[e^{\beta x/2 - \beta^2\zeta/4}u(x,\zeta)\right], \tag{B-21}$$

$$= e^{\beta(x-x^*(\tau))/2 - \beta^2\zeta/4}u(x - x^*(\tau),\zeta). \tag{B-22}$$

The relation (B-22) is obtained by the following proposition.

Proposition 3. *The evolution operator $e^{c(\tau)\frac{\partial}{\partial x}}$ satisfies the relation*

$$e^{c(\tau)\frac{\partial}{\partial x}} f(x) = f(x + c(\tau)). \tag{B-23}$$

Proof: Using Taylor series expansion, $f(x + c(\tau))$ can be expressed as

$$\begin{aligned} f(x + c(\tau)) &= f(x) + f'(x)(c(\tau)) + \frac{1}{2!} f''(x)(c(\tau))^2 + \cdots, \\ &= \sum_{n=0}^{\infty} \frac{1}{n!} (c(\tau))^n \frac{\partial^n f(x)}{\partial x^n} = \left[\sum_{n=0}^{\infty} \frac{c(\tau)^n}{n!} \frac{\partial^n}{\partial x^n} \right] f(x), \\ &= e^{c(\tau)\frac{\partial}{\partial x}} f(x). \end{aligned} \tag{B-24}$$

■

Next, we substitute boundary condition (18) into (B-22) and so obtain the zero boundary condition for u as[13]

$$u(0, \zeta) = 0. \tag{B-25}$$

and the initial condition for $\bar{P}_\beta(y) = 1$ at $\tau = 0$ yield

$$\bar{P}_\beta(y) = 1 = e^{\beta y} \widetilde{u}(y). \tag{B-26}$$

From (B-25), we note that the zero boundary condition is fulfilled, hence, we can apply the solution for the heat equation (A-5) to obtain the solution for $\bar{P}_\beta$ via the relation (B-22). Then, we substitute (B-26) and (B-22) into the solution for the heat equation (A-5), to obtain

$$e^{-\beta(x - x^*(\tau)) + \beta^2 \zeta/2} \bar{P}_\beta(x, \tau) = \int_{-\infty}^{0} \widetilde{g}(x - x^*(\tau), y; \zeta) e^{-\beta y} \bar{P}_\beta(y) dy. \tag{B-27}$$

Rearranging (B-27) and comparing to equation (20), we obtain

$$f_\beta(x, y, \tau) = e^{\beta[x - y - x^*(\tau)] - \beta^2 \zeta/2} \widetilde{g}(x - x^*(\tau), y; \zeta). \tag{B-28}$$

[13]We note that

$$\bar{P}_\beta(x^*(\tau), \tau) = 0 = e^{\beta \cdot 0 - \beta^2 \zeta/2} \widetilde{u}(0, \zeta).$$

Appendix C. The Method of Images in a Two-Dimensional Situation

Consider the two-dimensional heat equation

$$\frac{\partial u}{\partial \tau} = \frac{1}{2}\frac{\partial^2 u}{\partial x_1^2} + \rho_{12}\frac{\partial^2 u}{\partial x_1 \partial x_2} + \frac{1}{2}\frac{\partial^2 u}{\partial x_2^2}, \tag{C-1}$$

where x_1 and x_2 are unrestricted in the region $x_1, x_2 \in (-\infty, \infty)$. Its solution is known to be of the form

$$u(x_1, x_2, \tau) = \int_{-\infty}^{\infty}\int_{-\infty}^{\infty} g(x_1, x_2, y_1, y_2; \tau) u(y_1, y_2) dy_1 dy_2. \tag{C-2}$$

where $u(y_1, y_2)$ is the initial condition function and g is the bivariate transition probability density function for transition from y_1, y_2 to x_1, x_2 during a period of time τ, and has the form expressed in equation (15).[14]

The zero boundary conditions are imposed at $x_1 = 0$ and $x_2 = 0$, and require that

$$u(0, x_2, \tau) = 0, \tag{C-3}$$

$$u(x_1, 0, \tau) = 0, \tag{C-4}$$

and the region of interest for the solution is given by $x_1, x_2 \in (\infty, 0)$. The solution of the partial differential equation (C-1) subject to the boundary conditions (C-3) and (C-4) may be expressed as

$$u(x_1, x_2, \tau) = \int_{-\infty}^{0}\int_{-\infty}^{0} \widetilde{g}(x_1, x_2, y_1, y_2; \tau) u(y_1, y_2) dy_1 dy_2, \tag{C-5}$$

where $\widetilde{g}$ is the bivariate transition probability density function for the restricted process.

Applying the method of images approach, the solution for the density function $\widetilde{g}$ is a linear combinations of density functions g (for the unrestricted process) in such a way that their net effect cancels out at the barriers $x_1 = 0$ and $x_2 = 0$, then as a result the boundary conditions (C-3)-(C-4) are satisfied. To illustrate this concept, imagine there is a "source" density function

[14]More discussions, for example the multivariate continuous distributions can be found in Albanese & Campolieti (2006) Chapter 1.3.

(say g^0) located in the physical region[15] at the position (y_1^0, y_2^0) in the lower left hand quadrant (that is $g^0 = g^0(x_1, x_2, y_1^0, y_2^0; \tau)$), then we introduce an "image" density function (say g^1) in the nonphysical region at the position (y_1^1, y_2^1) in the lower right hand quadrant (that is $g^1 = g^1(x_1, x_2, y_1^1, y_2^1; \tau)$), such that the net effect of the two g functions cancel at the barrier $x_1 = 0$ as shown in Figure 9.

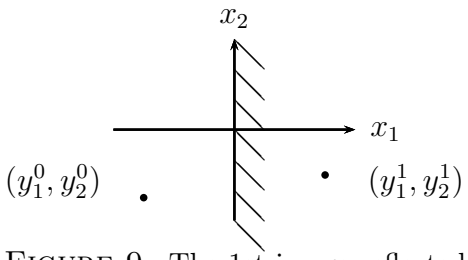

FIGURE 9. The 1st image reflected in $x_1 = 0$.

To determine (y_1^1, y_2^1), we consider the linear combination which in this case is given by

$$g^0(x_1, x_2 y_1^0, y_2^0; \tau) - g^1(x_1, x_2 y_1^1, y_2^1; \tau). \tag{C-6}$$

We require the combination in (C-6) to be zero at $x_1 = 0$, that is

$$g^0(0, x_2, y_1^0, y_2^0; \tau) - g^1(0, x_2, y_1^1, y_2^1; \tau) = 0. \tag{C-7}$$

Substituting equation (51) into (C-7), we see that the zero boundary condition at $x_1 = 0$ is satisfied provided that

$$\begin{aligned} &(0 - y_1^0)^2 - 2\rho_{12}(0 - y_1^0)(x_2 - y_2^0) + (x_2 - y_2^0)^2 \\ &= (0 - y_1^1)^2 - 2\rho_{12}(0 - y_1^1)(x_2 - y_2^1) + (x_2 - y_2^1)^2. \end{aligned} \tag{C-8}$$

Rearranging this expression, we obtain

$$x_2\phi + \alpha = 0, \tag{C-9}$$

[15]By the physical region we mean the region $-\infty < x_1 < 0$, $-\infty < x_2 < 0$.

where

$$\phi = 2(\rho_{12}y_1^0 - \rho_{12}y_1^1 - y_2^0 + y_2^1), \tag{C-10}$$

$$\alpha = (y_1^0)^2 - (y_1^1)^2 - 2\rho_{12}y_1^0y_2^0 + 2\rho_{12}y_1^1y_2^1 + (y_2^0)^2 - (y_2^1)^2. \tag{C-11}$$

In order that (C-9) hold for all x_2, it must be the case that $\phi = 0$ and $\alpha = 0$ hold simultaneously, in other words if

$$2(\rho_{12}y_1^0 - \rho_{12}y_1^1 - y_2^0 + y_2^1) = 0, \tag{C-12}$$

$$(y_1^0)^2 - (y_1^1)^2 - 2\rho_{12}y_1^0y_2^0 + 2\rho_{12}y_1^1y_2^1 + (y_2^0)^2 - (y_2^1)^2 = 0. \tag{C-13}$$

Solving (C-12) and (C-13) for y_1^1 and y_2^1, we obtain

$$y_1^1 = -y_1^0, \tag{C-14}$$

$$y_2^1 = y_2^0 - 2\rho_{12}y_1^0. \tag{C-15}$$

In the two-dimensional situation, there is also a barrier at $x_2 = 0$ and it is easy to verify that

$$g^0(x_1, 0, y_1^0, y_2^0; \tau) - g^1(x_1, 0, y_1^1, y_2^1; \tau) \neq 0. \tag{C-16}$$

Thus, we need to introduce another density function in the nonphysical region (say g^2) at the position (y_1^2, y_2^2) in the upper right hand quadrant (that is $g^2 = g^2(x_1, x_2, y_1^2, y_2^2; \tau)$, see Figure 10), such that it cancels out the effect of the image g^1 at $x_2 = 0$, that is, we require

$$g^1(x_1, 0, y_1^1, y_2^1; \tau) - g^2(x_1, 0, y_1^2, y_2^2; \tau) = 0. \tag{C-17}$$

To determine the vales of (y_1^2, y_2^2), we solve (C-17) similar to the way (C-8) was solved to obtain

$$y_2^2 = -y_2^1, \tag{C-18}$$

$$y_1^2 = y_1^1 - 2\rho_{12}y_2^1. \tag{C-19}$$

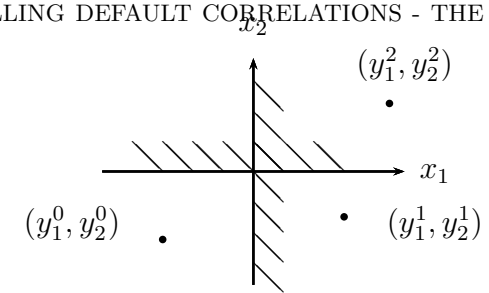

FIGURE 10. The 2nd image reflected in $x_2 = 0$.

However the introduction of the image density function g^2 will perturb the boundary condition at $x_1 = 0$[16]. So in order to cancel out this impact we need to introduce a third density function g^3 at (y_1^3, y_2^3) in the upper left hand quadrant as shown in Figure 11. In order to satisfy the boundary condition at $x_1 = 0$ we require

$$g^2(0, x_2, y_1^2, y_2^2; \tau) - g^3(0, x_2, y_1^3, y_2^3; \tau) = 0. \tag{C-20}$$

Solving equation (C-20) similarly to the way equation (C-8) was solved to obtain

$$y_1^3 = -y_1^2, \tag{C-21}$$

$$y_2^3 = y_2^2 - 2\rho_{12} y_1^2. \tag{C-22}$$

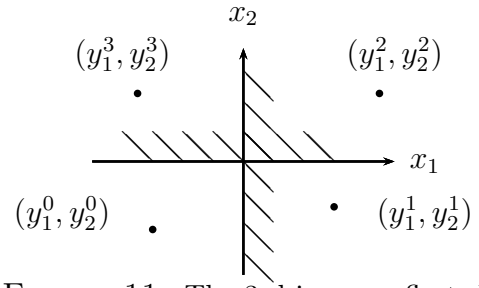

FIGURE 11. The 3rd image reflected in $x_1 = 0$.

Of course the introduction of density function g^3 could potentially perturb the boundary condition at $x_2 = 0$. However in the case $\rho_{12} = 0$ it turns out that the primary source at (y_1^0, y_2^0) and the image density functions g^1, g^2 and g^3 all balance each other such that the desired

[16]It is readily confirmed that

$$g^1(0, x_2, y_1^1, y_2^1; \tau) - g^2(0, x_2, y_1^2, y_2^2; \tau) \neq 0$$

boundary conditions at $x_1 = 0$ and $x_2 = 0$ are preserved. One can view this as the fact that if one were to obtain a fourth image g^4, the reflection of g^3 in $x_2 = 0$, it would be precisely the primary source (that is it turns out that $y_1^4 = y_1^0$, $y_2^4 = y_2^0$). Of course, in the method of images approach, an image cannot in fact be located in the region of interest (or the physical region), where the source is located. Thus for the case in which $\rho_{12} = 0$, the solution for $\widetilde{g}$ is the linear combination of the density functions g^0, g^1, g^2 and g^3, namely

$$\begin{aligned}\widetilde{g}(x_1, x_2, y_1^0, y_2^0; \tau) &= g^0(x_1, x_2, y_1^0, y_2^0; \tau) - g^1(x_1, x_2, y_1^1, y_2^1; \tau) \\ &\quad + g^2(x_1, x_2, y_1^2, y_2^2; \tau) - g^3(x_1, x_2, y_1^3, y_2^3; \tau), \end{aligned} \tag{C-23}$$

which satisfies $\widetilde{g}(0, x_2, y_1^0, y_2^0; \tau) = \widetilde{g}(x_1, 0, y_1^0, y_2^0; \tau) = 0$.

For general values of $\rho_{12} \in (-1, 1)$, we need to reflect successively more than three times in a set of mirrors located at lines from the origin in the image region in such a way that the "loop closes", and thus we would obtain after m reflections a set of m images such that the $(m+1)^{\text{st}}$ image would be the original source term. These m image terms just balance each other in such a way that the desired boundary conditions at $x_1 = 0$ and $x_2 = 0$ are preserved. In fact it turns out that only for specific values of ρ_{12} will the "loop close" after a finite number of reflections as shown in Appendix E, which also shows how to locate the set of reflecting mirrors. The values of ρ_{12} (rounded to 3 decimal places) that result in a "closed-loop" are shown in Table 1.

Dropping the superscripts in g^0 and (y_1^0, y_2^0), the solution for the density function $\widetilde{g}$ appearing in equation (C-5) may be written

$$\widetilde{g}(x_1, x_2, y_1, y_2; \tau) = g(x_1, x_2, y_1, y_2; \tau) + \sum_{k=1}^{m} (-1)^k g^k(x_1, x_2, y_1^k, y_2^k; \tau), \tag{C-24}$$

where m is the total number of images used to form the closed-loop in such a way that the desired boundary conditions (C-3)-(C-4) are preserved. Here y_1^k and y_2^k are obtained recursively from the relations between successive images as shown in equations (54)-(56) (for Y_1^k and Y_2^k replacing by y_1^k and y_2^k. Note that equations (54)-(56) are derived in the same way as equations (C-14)-(C-15), (C-18)-(C-19) and (C-21)-(C-22) were derived.

Appendix D. The Derivation of Equation (50)

Proposition 4. *The solution to the partial differential equation* (43) *with constant coefficients given in* (49) *may be written*

$$\bar{P}(X_1, X_2, \tau) \;=\; e^{\eta_1 X_1 + \eta_2 X_2 + \xi\tau} u(X_1, X_2, \tau), \tag{D-1}$$

where η_1, η_2 *and* ξ *are constants given by* (52)-(53)*, and* $u(X_1, X_2, \tau)$ *satisfies the two-dimensional heat equation* (C-1) *(with* X_1 *and* X_2 *replaced by* x_1 *and* x_2*).*

Proof: Define $\bar{P}$ such that $\bar{P}(X_1, X_2, \tau) = e^{\eta_1 X_1 + \eta_2 X_2}\widetilde{P}(X_1, X_2, \tau)$, where the η_1 and η_2 are to be chosen in a "convenient" way. We calculate

$$\begin{aligned}
\frac{\partial \bar{P}}{\partial \tau} &= e^{\eta_1 X_1 + \eta_2 X_2}\frac{\partial \widetilde{P}}{\partial \tau}, \\
\frac{\partial \bar{P}}{\partial X_i} &= e^{\eta_1 X_1 + \eta_2 X_2}\left[\eta_i \widetilde{P} + \frac{\partial \widetilde{P}}{\partial X_i}\right], \; (i = 1, 2) \\
\frac{\partial^2 \bar{P}}{\partial X_i^2} &= e^{\eta_1 X_1 + \eta_2 X_2}\left[\eta_i^2 \widetilde{P} + 2\eta_i \frac{\partial \widetilde{P}}{\partial X_i} + \frac{\partial^2 \widetilde{P}}{\partial X_i^2}\right], \; (i = 1, 2) \\
\frac{\partial^2 \bar{P}}{\partial X_1 \partial X_2} &= e^{\eta_1 X_1 + \eta_2 X_2}\left[\eta_1\eta_2 \widetilde{P} + \eta_2 \frac{\partial \widetilde{P}}{\partial X_1} + \eta_1 \frac{\partial \widetilde{P}}{\partial X_2} + \frac{\partial^2 \widetilde{P}}{\partial X_1 \partial X_2}\right].
\end{aligned} \tag{D-2}$$

Then equation (43) becomes

$$\begin{aligned}
\frac{\partial \widetilde{P}}{\partial \tau} \;=\; & \frac{1}{2}\frac{\partial^2 \widetilde{P}}{\partial X_1^2} + \rho_{12}\frac{\partial^2 \widetilde{P}}{\partial X_1 \partial X_2} + \frac{1}{2}\frac{\partial^2 \widetilde{P}}{\partial X_2^2} + \left[\eta_1 + \rho_{12}\eta_2 + \gamma_1\right]\frac{\partial \widetilde{P}}{\partial X_1} + \left[\eta_2 + \rho_{12}\eta_1 + \gamma_2\right]\frac{\partial \widetilde{P}}{\partial X_2} \\
& + \left[\frac{1}{2}\eta_1^2 + \frac{1}{2}\eta_2^2 + \rho_{12}\eta_1\eta_2 + \gamma_1\eta_1 + \gamma_2\eta_2\right]\widetilde{P}.
\end{aligned} \tag{D-3}$$

We may eliminate the $\partial\widetilde{P}/\partial X_1$ terms and $\partial\widetilde{P}/\partial X_2$ by choosing

$$\eta_1 + \rho_{12}\eta_2 + \gamma_1 = 0, \text{ and } \eta_2 + \rho_{12}\eta_1 + \gamma_2 = 0, \tag{D-4}$$

the simultaneous solution of which yields equations (52).

With these choices of η_1 and η_2 equation (D-3) reduce to

$$\frac{\partial \widetilde{P}}{\partial \tau} = \frac{1}{2}\frac{\partial^2 \widetilde{P}}{\partial X_1^2} + \rho_{12}\frac{\partial^2 \widetilde{P}}{\partial X_1 \partial X_2} + \frac{1}{2}\frac{\partial^2 \widetilde{P}}{\partial X_2^2} + \xi \widetilde{P}, \tag{D-5}$$

where, by use of equation (52) we obtained equation (53).

Next, we define u such that

$$\widetilde{P}(X_1, X_2, \tau) = e^{\xi\tau} u(X_1, X_2, \tau), \tag{D-6}$$

and calculate

$$\begin{aligned}
\frac{\partial \widetilde{P}}{\partial \tau} &= e^{\xi\tau}\left[\xi u + \frac{\partial u}{\partial \tau}\right], \\
\frac{\partial \widetilde{P}}{\partial X_i} &= e^{\xi\tau}\frac{\partial u}{\partial X_i}, \ (i = 1, 2) \\
\frac{\partial^2 \widetilde{P}}{\partial X_i^2} &= e^{\xi\tau}\frac{\partial^2 u}{\partial X_i^2}, \ (i = 1, 2) \\
\frac{\partial^2 \widetilde{P}}{\partial X_1 \partial X_2} &= e^{\xi\tau}\frac{\partial^2 u}{\partial X_1 \partial X_2}.
\end{aligned} \tag{D-7}$$

It then follows that $u(X_1, X_2, \tau)$ satisfies the two-dimensional heat equation (C-1) for X_1 and X_2 replacing by x_1 and x_2.

■

Appendix E. The Number of Images and the Correlation Coefficient ρ_{12}

The method of images applied in Appendix D for the two absorbing barriers case is only valid for certain values of the correlation coefficient ρ_{12}. This appendix demonstrates the relationship between the total number of images required to form a "closed-loop" and the corresponding value of the correlation coefficient ρ_{12}.

In order to obtain the number of images that form the closed-loop, it is convenient to transform the volatility adjusted correlated log-leverage ratio variables x_1 and x_2 to the uncorrelated

variables z_1, z_2 by setting

$$z_2 = x_2, \tag{E-1}$$

$$z_1 = \frac{1}{\sqrt{1-\rho_{12}^2}}(x_1 - \rho_{12}x_2). \tag{E-2}$$

In order to eliminate the mixed derivative term from the heat equation (C-1), we make the transformation

$$u(x_1, x_2, \tau) = \widetilde{u}(z_1(x_1, x_2), z_2(x_2), \tau), \tag{E-3}$$

using the change of variables defined in equations (E-1)-(E-2).

Since

$$\frac{\partial z_2}{\partial x_1} = 0 \quad ; \quad \frac{\partial z_2}{\partial x_2} = 1$$
$$\frac{\partial z_1}{\partial x_1} = \alpha \quad ; \quad \frac{\partial z_1}{\partial x_2} = -\alpha\rho,$$

with $\alpha = 1/\sqrt{1-\rho^2}$, we have

$$\begin{aligned}
\frac{\partial u}{\partial x_1} &= \alpha\frac{\partial}{\partial z_1}\widetilde{P} \\
\frac{\partial^2 u}{\partial x_1^2} &= \alpha^2\frac{\partial^2}{\partial z_1^2}\widetilde{u} \\
\frac{\partial u}{\partial x_2} &= \left[\frac{\partial}{\partial z_2} - \alpha\rho\frac{\partial}{\partial z_1}\right]\widetilde{u} \\
\frac{\partial^2 u}{\partial x_2^2} &= \left[\frac{\partial^2}{\partial z_2^2} - 2\alpha\rho\frac{\partial^2}{\partial z_1\partial z_2} + (\alpha\rho)^2\frac{\partial^2}{\partial z_1^2}\right]\widetilde{u} \\
\frac{\partial^2 u}{\partial x_1\partial x_2} &= \left[\alpha\frac{\partial^2}{\partial z_1\partial z_2} - \alpha^2\rho\frac{\partial^2}{\partial z_1^2}\right]\widetilde{u}.
\end{aligned} \tag{E-4}$$

Substituting (E-4) into (C-1), yields

$$\begin{aligned}\frac{\partial \widetilde{u}}{\partial \tau} =& \frac{1}{2}\left[\alpha^2\frac{\partial^2}{\partial z_1^2}\right]\widetilde{u} + \frac{1}{2}\left[\frac{\partial^2}{\partial z_2^2} - 2\alpha\rho\frac{\partial^2}{\partial z_1 \partial z_2} + (\alpha\rho)^2\frac{\partial^2}{\partial z_1^2}\right]\widetilde{u} + \rho\left[\alpha\frac{\partial^2}{\partial z_1 \partial z_2} - \alpha^2\rho\frac{\partial^2}{\partial z_1^2}\right]\widetilde{u} \\ =& \quad \frac{1}{2}\alpha^2\frac{\partial^2 \widetilde{u}}{\partial z_1^2} + \frac{1}{2}\frac{\partial^2 \widetilde{u}}{\partial z_2^2} - \alpha\rho\frac{\partial^2 \widetilde{u}}{\partial z_1 \partial z_2} + \frac{1}{2}(\alpha\rho)^2\frac{\partial^2 \widetilde{u}}{\partial z_1^2} + \rho\alpha\frac{\partial^2 \widetilde{u}}{\partial z_1 \partial z_2} - (\rho\alpha)^2\frac{\partial^2 \widetilde{u}}{\partial z_1^2} \\ =& \left[\frac{1}{2}\alpha^2 + \frac{1}{2}(\alpha\rho)^2 - (\rho\alpha)^2\right]\frac{\partial^2 \widetilde{u}}{\partial z_1^2} + \frac{1}{2}\frac{\partial^2 \widetilde{u}}{\partial z_2^2},\end{aligned}$$

rearranging the term in the bracket on the right hand side $\left[\frac{1}{2}\alpha^2 + \frac{1}{2}(\alpha\rho)^2 - (\rho\alpha)^2\right]$ we find that it equals $\frac{1}{2}$, therefore we obtain

$$\frac{\partial \widetilde{u}}{\partial \tau} = \frac{1}{2}\frac{\partial^2 \widetilde{u}}{\partial z_1^2} + \frac{1}{2}\frac{\partial^2 \widetilde{u}}{\partial z_2^2}. \tag{E-5}$$

The absorbing barriers $x_1 = 0$ and $x_2 = 0$ determine the barriers of the uncorrelated variables, which become

$$z_2 = 0, \tag{E-6}$$

$$z_1 = -\frac{\rho_{12}}{\sqrt{1-\rho_{12}^2}} z_2. \tag{E-7}$$

The transformation of the barriers is also illustrated in Figure 12, and we note that the barrier for z_1 depends on z_2 as well.

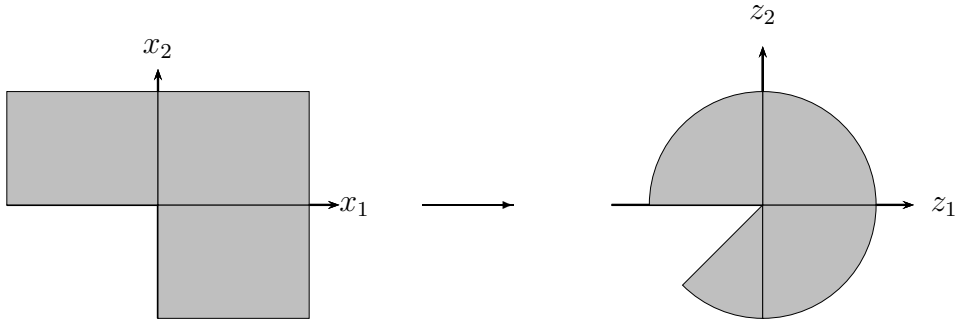

FIGURE 12. The transformation of the barriers.

Since x_1 and x_2 are defined in the region $x_1, x_2 \in (-\infty, 0) \times (-\infty, 0)$ (represented by the non-shaded region in the left hand panel in Figure 13), then for z_1, z_2 the regions of definition are

$z_2 \in (-\frac{\sqrt{1-\rho_{12}^2}}{\rho_{12}} z_1, 0)$ and $z_1 \in (-\infty, -\frac{\rho_{12}}{\sqrt{1-\rho_{12}^2}} z_2)$, and there is an angle ϕ' (represented by the angle ϕ' in the right hand panel in Figure 13) between the two planes of the barrier $z_2 = 0$ and $z_1 = -\frac{\rho_{12}}{\sqrt{1-\rho_{12}^2}} z_2$.

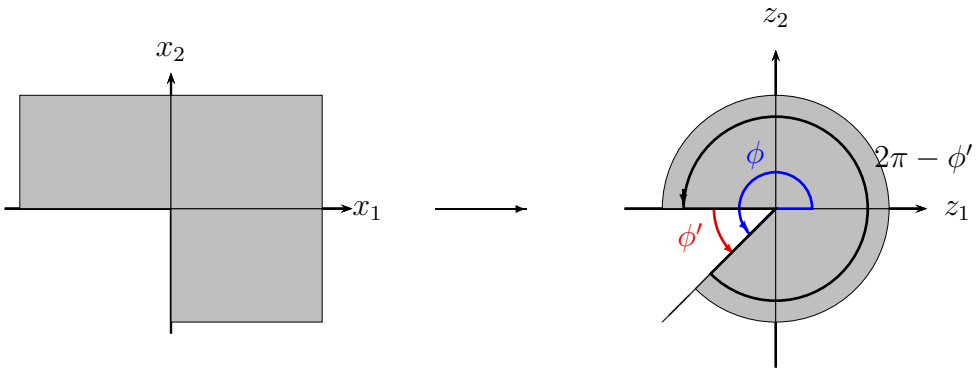

FIGURE 13. The non-shaded area in the left hand panel represents the restricted region in x_1, x_2 co-ordinates. After the transformation, the wedge shaped non-shaded region forming the angle ϕ' in the right hand panel represents the restricted region in z_1, z_2 co-ordinates.

In the ensuing discussion it is important to distinguish between the polar angle ϕ (measured clockwise from the positive z_1 axis) and the angle ϕ' (measured clockwise from the negative z_1 axis), as shown in the right panel of Figure 13, and which are related by $\phi' = \phi - \pi$.

Next, we relate the angle ϕ' to the correlation coefficient ρ_{12}. By simple trigonometry for a point (z_1, z_2) in the line $z_1 = -\frac{\rho_{12}}{\sqrt{1-\rho_{12}^2}} z_2$, we have

$$z_1 = R \cos \phi, \tag{E-8}$$

where R is the radius defined as $R = \sqrt{z_1^2 + z_2^2}$.

Equation (E-8) may be written as

$$z_1 = \sqrt{z_1^2 + z_2^2} \cos \phi, \tag{E-9}$$

which by use of the relation (E-7) becomes

$$z_1^2 = \left(z_1^2 + \frac{1-\rho_{12}^2}{\rho_{12}^2} z_1^2\right) \cos^2 \phi, \tag{E-10}$$

from which we obtain

$$\rho_{12} = \pm \cos\phi. \tag{E-11}$$

From (E-11), we note that the condition $-1 < \rho_{12} < 1$ determines region of ϕ which is $\pi < \phi < 2\pi$, hence the values of ϕ' satisfy $0 < \phi' < \pi$ (since $\phi' = \phi - \pi$). If $\rho_{12} < 0$ then $0 < \phi' < \frac{\pi}{2}$, if $\rho_{12} = 0$ then $\phi' = \frac{\pi}{2}$ and if $\rho_{12} > 0$ then $\frac{\pi}{2} < \phi' < \pi$ as illustrated in Figure 14:

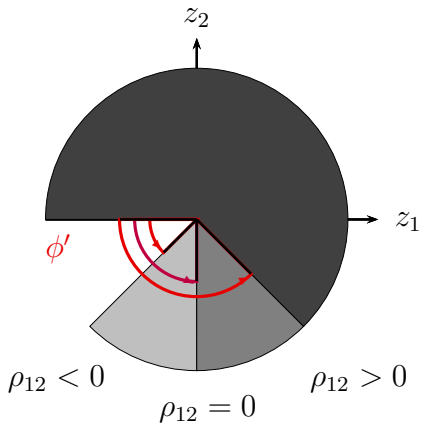

FIGURE 14. The relationship between the correlation coefficient ρ_{12} and the angle ϕ'.

Note that we can only form the closed loop of images for values of the angle ϕ' that divide the angle $(2\pi - \phi')$ into an exact integer number. Denote by m the number of images, then in order to form the closed-loop, the integer m must be related to the angle ϕ' by

$$m = \frac{2\pi - \phi'}{\phi'}. \tag{E-12}$$

We stress that m must be a positive integer, also the values of m that satisfy this relation are the odd integers starting from 3. These values of m via equation (E-12), will then determine the values of ρ_{12} for which the method of images can be applied.

For example, given $\phi' = \frac{\pi}{2}$ (at which $\rho_{12} = 0$), we require $m = 3$ images to form the closed-loop (see Figure 15), that is if we successively reflect a point in the physical region in the mirrors at the lines radiating from the origin at polar angles $\phi = \frac{3\pi}{2}$, $\phi = 0$, $\phi = \frac{\pi}{2}$ and $\phi = \pi$ we will arrive back at the original point.

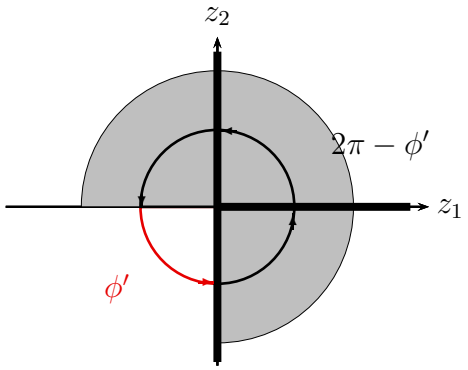

FIGURE 15. To form the closed-loop for the angle $\phi' = \frac{\pi}{2}$, three images are required.

Next consider $\phi' = \frac{\pi}{3}$ (at which $\rho_{12} = -0.5$) illustrated in Figure 16. The lines bounding the image region (shaded in Figure 16) lie between the polar angles $\phi = \pi$ and $\phi = \frac{4\pi}{3}$ in the clockwise direction. So the angle separating the two defining lines is $\frac{5\pi}{3}$ $(= 2\pi - \phi')$, which can be divided precisely into five regions separated by lines at an angle of $\pi/3$ apart, as shown in Figure 16. These lines are five mirrors in which the point in the physical region is successively reflected to give the five image points. A further reflection in the line $\phi = \pi$ would take us back to the original point, thus completing the loop. Figure 17 illustrates the situation for $\phi' = \frac{\pi}{4}$ (at which $\rho_{12} = -0.707$) for which seven mirrors, resulting in seven images, are required to form a closed loop.

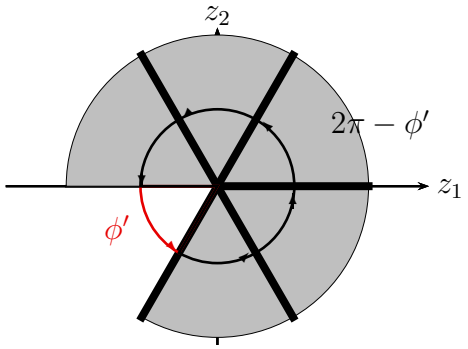

FIGURE 16. To form a closed loop for the angle $\phi' = \frac{\pi}{3}$, five images are required.

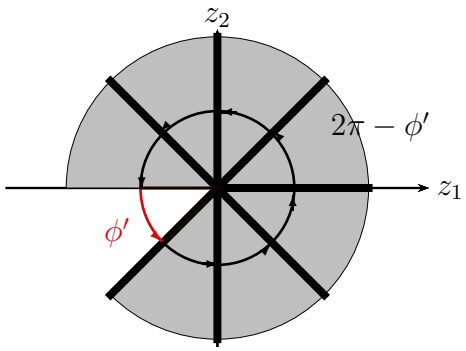

FIGURE 17. To form a closed loop for the angle $\phi' = \frac{\pi}{4}$, seven images are required.

We can now see that the general relationship between the value of ρ_{12} and the member of images m needed to form a closed-loop is obtained by substituting (E-12) into (E-11), using the relation $\phi' = \phi - \pi$, to yield

$$\rho_{12} = -\cos\big(\frac{2\pi}{m+1}\big), \tag{E-13}$$

for $m = 3, 5, 7, \ldots$. The corresponding values of ρ_{12} are summarized in Table 1.

Appendix F. The Derivation of Equation (63)

Proposition 5. *The partial differential equation* (58) *can be transformed by setting*

$$\bar{P}_{\boldsymbol{\beta}}(X_1, X_2, \tau) \;=\; e^{-X_1^*(\tau)\frac{\partial}{\partial X_1} - X_2^*(\tau)\frac{\partial}{\partial X_2}}\widetilde{P}(X_1, X_2, \tau), \tag{F-1}$$

where the $X_i^*(\tau)$ *is given by*

$$X_i^*(\tau) = -\int_0^\tau \gamma_i(v)dv - \beta_i\tau, \;\; (i = 1, 2), \tag{F-2}$$

and $\widetilde{P}(X_1, X_2, \tau)$ *satisfies the partial differential*

$$\frac{\partial \widetilde{P}}{\partial \tau} \;=\; \frac{1}{2}\frac{\partial^2 \widetilde{P}}{\partial X_1^2} + \rho_{12}\frac{\partial^2 \widetilde{P}}{\partial X_1 \partial X_2} + \frac{1}{2}\frac{\partial^2 \widetilde{P}}{\partial X_2^2} - \beta_1\frac{\partial \widetilde{P}}{\partial X_1} - \beta_2\frac{\partial \widetilde{P}}{\partial X_2}. \tag{F-3}$$

Proof: Apply the Baker-Campbell-Hausdorff formula in Appendix B, and after some algebraic manipulations, we obtain

$$\begin{aligned}
\frac{\partial \bar{P}_{\boldsymbol{\beta}}}{\partial \tau} &= e^{-X_1^*(\tau)\frac{\partial}{\partial X_1}-X_2^*(\tau)\frac{\partial}{\partial X_2}}\left[\frac{\partial \widetilde{P}}{\partial \tau}-\frac{\partial X_1^*(\tau)}{\partial \tau}\frac{\partial \widetilde{P}}{\partial X_1}-\frac{\partial X_2^*(\tau)}{\partial \tau}\frac{\partial \widetilde{P}}{\partial X_2}\right], \\
\frac{\partial \bar{P}_{\boldsymbol{\beta}}}{\partial X_i} &= e^{-X_1^*(\tau)\frac{\partial}{\partial X_1}-X_2^*(\tau)\frac{\partial}{\partial X_2}}\frac{\partial \widetilde{P}}{\partial X_i},\ (i=1,2), \\
\frac{\partial^2 \bar{P}_{\boldsymbol{\beta}}}{\partial X_i^2} &= e^{-X_1^*(\tau)\frac{\partial}{\partial X_1}-X_2^*(\tau)\frac{\partial}{\partial X_2}}\frac{\partial^2 \widetilde{P}}{\partial X_i^2},\ (i=1,2), \\
\frac{\partial^2 \bar{P}_{\boldsymbol{\beta}}}{\partial X_1 \partial X_2} &= e^{-X_1^*(\tau)\frac{\partial}{\partial X_1}-X_2^*(\tau)\frac{\partial}{\partial X_2}}\frac{\partial^2 \widetilde{P}}{\partial X_1 \partial X_2}.
\end{aligned} \tag{F-4}$$

Then equation (58) becomes

$$\begin{aligned}
\frac{\partial \widetilde{P}}{\partial \tau}-\frac{\partial X_1^*(\tau)}{\partial \tau}\frac{\partial \widetilde{P}}{\partial X_1}-\frac{\partial X_2^*(\tau)}{\partial \tau}\frac{\partial \widetilde{P}}{\partial X_2} &= \frac{1}{2}\frac{\partial^2 \widetilde{P}}{\partial X_1^2}+\rho_{12}\frac{\partial^2 \widetilde{P}}{\partial X_1 \partial X_2}+\frac{1}{2}\frac{\partial^2 \widetilde{P}}{\partial X_2^2} \\
&\quad +\gamma_1(\tau)\frac{\partial \widetilde{P}}{\partial X_1}+\gamma_2(\tau)\frac{\partial \widetilde{P}}{\partial X_2}.
\end{aligned} \tag{F-5}$$

Define $X_i^*(\tau)$ for $i=1,2$ by setting

$$-\frac{\partial X_i^*(\tau)}{\partial \tau}=\gamma_i(\tau)+\beta_i, \tag{F-6}$$

so that we obtained the dynamics of β_i as shown in (61). Hence, the partial differential equation (F-5) becomes

$$\begin{aligned}
&\frac{\partial \widetilde{P}}{\partial \tau}+\gamma_1(\tau)\frac{\partial \widetilde{P}}{\partial X_1}+\beta_1\frac{\partial \widetilde{P}}{\partial X_1}+\gamma_2(\tau)\frac{\partial \widetilde{P}}{\partial X_2}+\beta_2\frac{\partial \widetilde{P}}{\partial X_2} \\
&\quad = \frac{1}{2}\frac{\partial^2 \widetilde{P}}{\partial X_1^2}+\rho_{12}\frac{\partial^2 \widetilde{P}}{\partial X_1 \partial X_2}+\frac{1}{2}\frac{\partial^2 \widetilde{P}}{\partial X_2^2}+\gamma_1(\tau)\frac{\partial \widetilde{P}}{\partial X_1}+\gamma_2(\tau)\frac{\partial \widetilde{P}}{\partial X_2},
\end{aligned} \tag{F-7}$$

which then turns out to be equation (F-3).

We note that the partial differential equation (F-3) can be further reduced to the two-dimensional heat equation u. We apply the Proposition 4 illustrated in Appendix D for the transformation. Simply replacing $\bar{P}$ by $\widetilde{P}$, and replacing the coefficients γ_i by $-\beta_i$ (for $i=1,2$), we obtain

$$\widetilde{P}(X_1,X_2,\tau) = e^{\bar{\eta}_1 X_1+\bar{\eta}_2 X_2+\bar{\xi}\tau}u(X_1,X_2,\tau), \tag{F-8}$$

where $\bar{\eta}_1$, $\bar{\eta}_2$ and $\bar{\xi}$ are constants given by (64)-(65), and $u(X_1, X_2, \tau)$ satisfies the two-dimensional heat equation (C-1) (with X_1 and X_2 replaced by x_1 and x_2).

■

Combing the transformation in (F-1) and (F-8), we have related (58) to the two-dimensional heat equation u in (C-1) (with τ replaced by ζ and x_1, x_2 by X_1, X_2) by

$$\begin{aligned} \bar{P}_{\boldsymbol{\beta}}(X_1, X_2, \tau) &= e^{-X_1^*(\tau)\frac{\partial}{\partial X_1} - X_2^*(\tau)\frac{\partial}{\partial X_2}} \left[e^{\bar{\eta}_1 X_1 + \bar{\eta}_2 X_2 + \bar{\xi}\tau} u(X_1, X_2, \tau) \right], & \text{(F-9)} \\ &= e^{\bar{\eta}_1[X_1 - X_1^*(\tau)] + \bar{\eta}_2[X_2 - X_2^*(\tau)] + \bar{\xi}\tau} u(X_1 - X_1^*(\tau), X_2 - X_2^*(\tau), \tau), & \text{(F-10)} \end{aligned}$$

Substitution of the zero boundary conditions (59) and (60) into (F-10) yields the boundary conditions for u as[17]

$$u(0, X_2 - X_2^*(\tau), \tau) = 0, \tag{F-11}$$

$$u(X_1 - X_1^*(\tau), 0, \tau) = 0. \tag{F-12}$$

The zero boundary conditions (F-11) - (F-12) for u occur when the value of the barriers are equal to zero, and fulfill the conditions in (C-3)-(C-4) (replacing the space variables x_i by $X_i - X_i^*(\tau)$). Therefore, the solution $\widetilde{g}$ in (C-24) can be applied to obtain the solution for $\bar{P}_{\boldsymbol{\beta}}$.

First, substitution of the initial condition $\bar{P}_{\boldsymbol{\beta}}(Y_1, Y_2) = 1$ with $X_1(0) = Y_1$ and $X_2(0) = Y_2$ into (F-10) to determines the initial condition of u, which is

$$\bar{P}_{\boldsymbol{\beta}}(Y_1, Y_2) = 1 = e^{\bar{\eta}_1 Y_1 + \bar{\eta}_2 Y_2} u(Y_1, Y_2). \tag{F-13}$$

Then, substitution equations (F-13) and (F-10) into equation (C-5), yields

$$\begin{aligned} & e^{-\bar{\eta}_1[X_1 - X_1^*(\tau)] - \bar{\eta}_2[X_2 - X_2^*(\tau)] - \bar{\xi}\tau} \bar{P}_{\boldsymbol{\beta}}(X_1, X_2, \tau) \\ &\quad = \int_{-\infty}^{0}\int_{-\infty}^{0} \widetilde{g}(X_1 - X_1^*(\tau), X_2 - X_2^*(\tau), Y_1, Y_2; \tau) e^{-\bar{\eta}_1 Y_1 - \bar{\eta}_2 Y_2} \bar{P}_{\boldsymbol{\beta}}(Y_1, Y_2) dY_1 dY_2, \end{aligned} \tag{F-14}$$

[17] We note that

$$\bar{P}_{\boldsymbol{\beta}}(X_1^*(\tau), X_2, \tau) = 0 = e^{\bar{\eta}_1 \cdot 0 + \bar{\eta}_2[X_2 - X_2^*(\tau)] + \bar{\xi}\tau} u(0, X_2 - X_2^*(\tau), \tau),$$
$$\bar{P}_{\boldsymbol{\beta}}(X_1, X_2^*(\tau), \tau) = 0 = e^{\bar{\eta}_1[X_1 - X_1^*(\tau)] + \bar{\eta}_2 \cdot 0) + \bar{\xi}\tau} u(X_1 - X_1^*(\tau), 0, \tau).$$

Substituting (C-24) into (F-14) and rearranging it, we obtained

$$\bar{P}_{\boldsymbol{\beta}}(X_1, X_2, \tau) = \int_{-\infty}^{0}\int_{-\infty}^{0} e^{\bar{\eta}_1[X_1 - X_1^*(\tau) - Y_1] + \bar{\eta}_2[X_2 - X_2^*(\tau) - Y_2] + \bar{\xi}\tau}\Big[g(X_1 - X_1^*(\tau), X_2 - X_2^*(\tau), Y_1, Y_2; \tau) + \sum_{k=1}^{m}(-1)^k g^k(X_1 - X_1^*(\tau), X_2 - X_2^*(\tau), Y_1^k, Y_2^k; \tau)\Big]\bar{P}_{\boldsymbol{\beta}}(Y_1, Y_2)dY_1 dY_2. \tag{F-15}$$

where Y_1^k, Y_2^k are given in (54)-(56).

Finally, by comparing equations (F-15) and (62), we obtained the solution of the joint transition probability density function as shown in (63).

The following proposition gives the proof of equation (F-10).

Proposition 6. *The expression*

$$e^{c_1(\tau)\frac{\partial}{\partial x_1} + c_2(\tau)\frac{\partial}{\partial x_2}} f(x_1, x_2), \tag{F-16}$$

may be written as

$$f(x_1 + c_1(\tau), x_2 + c_2(\tau)). \tag{F-17}$$

Proof: Using Taylor series expansion, $f(x_1 + c_1(\tau), x_2 + c_2(\tau))$

$$\begin{aligned} f(x_1 + c_1(\tau), x_2 + c_2(\tau)) &= \sum_{n=0}^{\infty}\sum_{m=0}^{\infty}\frac{1}{n!m!}\frac{\partial^n}{\partial x_1^n}\frac{\partial^m}{\partial x_2^m}[f(x_1, x_2)]c_1(\tau)^n c_2(\tau)^m, \\ &= \left[\sum_{n=0}^{\infty}\frac{c_1(\tau)^n}{n!}\frac{\partial^n}{\partial x_1^n}\right]\left[\sum_{m=0}^{\infty}\frac{c_2(\tau)^m}{m!}\frac{\partial^m}{\partial x_2^m}\right] f(x_1, x_2), \\ &= e^{c_1(\tau)\frac{\partial}{\partial x_1}} e^{c_2(\tau)\frac{\partial}{\partial x_2}} f(x_1, x_2). \end{aligned} \tag{F-18}$$

The last equality follows from repeated application of the definition (B-4).

■

Appendix G. The Numerical Implementation of Equations (57) and (66)

The solution for the joint survival probability (57) can be expressed in term of the cumulative bivariate normal distribution function $N_2(\cdot)$, which has the form

$$N_2(a,b,\rho) = \int_{-\infty}^{a}\int_{-\infty}^{b} n_2(u,v,\rho)dvdu, \tag{G-1}$$

where the bivariate normal density function is given by

$$n_2(a,b,\rho) \;=\; \frac{1}{2\pi\sqrt{1-\rho^2}}\exp\left(-\frac{u^2-2\rho uv+v^2}{2(1-\rho^2)}\right). \tag{G-2}$$

Consider (57) and rearrange it as

$$\begin{aligned} F(X_1,X_2,\tau) = &\int_{-\infty}^{0}\int_{-\infty}^{0} e^{\eta_1(X_1-Y_1)+\eta_2(X_2-Y_2)+\xi\tau} g(X_1,X_2,Y_1,Y_2;\tau)dY_1dY_2 \\ &+\sum_{k=1}^{m}(-1)^k\int_{-\infty}^{0}\int_{-\infty}^{0} e^{\eta_1(X_1-Y_1)+\eta_2(X_2-Y_2)+\xi\tau} g^k(X_1,X_2,Y_1^k,Y_2^k;\tau)dY_1dY_2. \end{aligned} \tag{G-3}$$

Substituting the expression of the density function (51) into (G-3), the first integral in equation (G-3) can be written as

$$e^{\eta_1X_1+\eta_2X_2+\xi\tau}\int_{-\infty}^{0}\int_{-\infty}^{0}\frac{1}{2\pi\tau\sqrt{1-\rho_{12}^2}}\exp\left(-\frac{\phi(Y_1,Y_2)}{2\tau(1-\rho_{12}^2)}\right)dY_1dY_2. \tag{G-4}$$

where

$$\phi(Y_1,Y_2) \;=\; AY_1^2+BY_2^2+CY_1+DY_2+EY_1Y_2+H, \tag{G-5}$$

and

$$\begin{aligned} A &= 1,\ B=1, \\ C &= 2[\eta_1\tau(1-\rho_{12}^2)-X_1+\rho_{12}X_2], \\ D &= 2[\eta_2\tau(1-\rho_{12}^2)-X_2+\rho_{12}X_1], \\ E &= -2\rho_{12}, \\ H &= X_1^2+X_2^2-2\rho_{12}X_1X_2. \end{aligned} \tag{G-6}$$

Then, equation (G-4) can be written in terms of the cumulative bivariate normal distribution function $N_2(\cdot)$ by the change of variables illustrated in Appendix H, hence (G-4) becomes

$$e^{\eta_1 X_1+\eta_2 X_2+\xi\tau}\sqrt{\frac{(1-\rho_{12}^2)}{AB(1-\widetilde{\rho}^2)}}\ \exp\left(-\frac{\widetilde{h}}{2\tau(1-\rho_{12}^2)}\right)\times N_2(\widetilde{a},\widetilde{b},\widetilde{\rho}), \tag{G-7}$$

where

$$\widetilde{\rho} = -\frac{E}{2\sqrt{AB}}, \tag{G-8}$$

$$\widetilde{a} = \sqrt{2(1-\widetilde{\rho}^2)}\ \widetilde{u}_1 = \sqrt{\frac{A}{\tau}}\left(\frac{C}{2A}-\frac{Eh_2}{4Ah_1}\right)\ \sqrt{\frac{1-\widetilde{\rho}^2}{1-\rho_{12}^2}}, \tag{G-9}$$

$$\widetilde{b} = \sqrt{2(1-\widetilde{\rho}^2)}\ \widetilde{v}_1 = \frac{1}{\sqrt{\tau}}\sqrt{1+\frac{E^2}{4Ah_1}}\ \frac{h_2}{2\sqrt{h_1}}\ \sqrt{\frac{1-\widetilde{\rho}^2}{1-\rho_{12}^2}}, \tag{G-10}$$

and

$$h_1 = B-\frac{E^2}{4A},\ h_2 = D-\frac{CE}{2A},\ \widetilde{h} = H-\frac{C^2}{4A}-\frac{h_2^2}{4h_1}. \tag{G-11}$$

Next we consider the second integral in equation (G-3). We note that it is convenient to rewrite Y_1^k and Y_2^k in terms of Y_1 and Y_2 by setting

$$Y_1^k = a_1^k Y_1 + b_1^k Y_2,\ Y_2^k = a_2^k Y_1 + b_2^k Y_2. \tag{G-12}$$

Substituting equations (G-12) into (54)-(56), we find that for $k>1$

$$\begin{aligned} a_1^k &= \begin{cases} -a_1^{k-1} & \text{for } k \text{ is odd,} \\ a_1^{k-1}-2\rho_{12}a_2^{k-1} & \text{for } k \text{ is even,} \end{cases} \\ a_2^k &= \begin{cases} a_2^{k-1}-2\rho_{12}a_1^{k-1} & \text{for } k \text{ is odd,} \\ -a_2^{k-1} & \text{for } k \text{ is even,} \end{cases} \\ b_1^k &= a_2^{k-1},\ b_2^k = a_1^{k-1}, \end{aligned} \tag{G-13}$$

whilst for $k=1$

$$\begin{aligned} a_1^1 &= -1\ ,\ b_1^1 = 0, \\ a_2^1 &= -2\rho_{12}\ ,\ b_2^1 = 1. \end{aligned} \tag{G-14}$$

Then, the second integral in equation (G-3) can be expressed as

$$\sum_{k=1}^{m}(-1)^k \int_{-\infty}^{0}\int_{-\infty}^{0} e^{\eta_1(X_1-Y_1)+\eta_2(X_2-Y_2)+\xi\tau} \times g^k\Big(X_1, X_2, (a_1^k Y_1 + b_1^k Y_2), (a_2^k Y_1 + b_2^k Y_2); \tau\Big) dY_1 dY_2. \tag{G-15}$$

Following steps analogous to those shown in Appendix H, this can be written in terms of $N_2(\cdot)$ as

$$e^{\eta_1 X_1+\eta_2 X_2+\xi\tau} \sum_{k=1}^{m}(-1)^k \sqrt{\frac{(1-\rho_{12}^2)}{A_k B_k(1-\widetilde{\rho}_k^2)}}\ \exp\left(-\frac{\widetilde{h}_k}{2\tau(1-\rho_{12}^2)}\right) \times N_2\big(\widetilde{a}_k, \widetilde{b}_k, \widetilde{\rho}_k\big). \tag{G-16}$$

The expressions for $\widetilde{\rho}_k$, $\widetilde{a}_k$, $\widetilde{b}_k$ and $\widetilde{h}_k$ are the same as in (G-8)-(G-11) but obtained by replacing A, B, C, D and E by

$$\begin{aligned}
A_k &= (a_1^k)^2 + (a_2^k)^2 - 2\rho_{12} a_1^k a_2^k, \\
B_k &= (b_1^k)^2 + (b_2^k)^2 - 2\rho_{12} b_1^k b_2^k, \\
C_k &= X_1(2\rho_{12} a_2^k - 2a_1^k) + X_2(2\rho_{12} a_1^k - 2a_2^k) + 2\eta_1\tau(1-\rho_{12}^2), \\
D_k &= X_1(2\rho_{12} b_2^k - 2b_1^k) + X_2(2\rho_{12} b_1^k - 2b_2^k) + 2\eta_2\tau(1-\rho_{12}^2), \\
E_k &= 2(a_1^k b_1^k + a_2^k b_2^k - \rho_{12} b_1^k a_2^k - \rho_{12} a_1^k b_2^k).
\end{aligned} \tag{G-17}$$

The case for the time varying coefficients

We consider the approximate solution for the joint survival probability in (66) after some algebraic manipulations, can be simplified to

$$\begin{aligned}
F_\beta(X_1, X_2, \tau) = &\int_{-\infty}^{0}\int_{-\infty}^{0} g(X_1 + d_1(\tau), X_2 + d_2(\tau), Y_1, Y_2; \tau) dY_1 dY_2 \\
&+ \sum_{k=1}^{m}(-1)^k \int_{-\infty}^{0}\int_{-\infty}^{0} g^k(X_1 + d_1(\tau), X_2 + d_2(\tau), Y_1^k, Y_2^k; \tau) e^{\beta_a^k Y_1 + \beta_b^k Y_2} dY_1 dY_2,
\end{aligned} \tag{G-18}$$

where

$$d_i(\tau) = \int_0^\tau \gamma_i(v) dv,\ (i = 1, 2), \tag{G-19}$$

and

$$\beta_a^k = \bar{\eta}_1(a_1^k - 1) + \bar{\eta}_2 a_2^k, \tag{G-20}$$

$$\beta_b^k = \bar{\eta}_1 b_1^k + \bar{\eta}_2(b_2^k - 1), \tag{G-21}$$

and the a^k's and b^k's are given in (G-13)-(G-14).

Applying the same procedures as in Appendix H, the first integral in (G-18) can be rewritten in terms of $N_2(\cdot)$ as

$$\sqrt{\frac{(1-\rho_{12}^2)}{AB(1-\widetilde{\rho}^2)}}\ \exp\left(-\frac{\widetilde{h}}{2\tau(1-\rho_{12}^2)}\right) \times N_2(\widetilde{a}, \widetilde{b}, \widetilde{\rho}). \tag{G-22}$$

The expressions for $\widetilde{\rho}$, $\widetilde{a}$, $\widetilde{b}$, h_1, h_2 and $\widetilde{h}$ are the same as in (G-8)-(G-11) after replacing C, D and H with

$$\begin{aligned} C &= 2(-\mathbb{X}_1 + \rho_{12}\mathbb{X}_2), \\ D &= 2(-\mathbb{X}_2 + \rho_{12}\mathbb{X}_1), \\ H &= \mathbb{X}_1^2 + \mathbb{X}_2^2 - 2\rho_{12}\mathbb{X}_1\mathbb{X}_2, \end{aligned} \tag{G-23}$$

and $\mathbb{X}_i = X_i + d_i(\tau)$ for $i = 1, 2$.

In a similar way to the calculation in the case of constant coefficients, we simplify the second integral in (G-18) by rewriting Y_1^k and Y_2^k in terms of Y_1 and Y_2 using the expressions in (G-12), and applying the same procedures used in Appendix H, we obtain

$$\sum_{k=1}^{m}(-1)^k\sqrt{\frac{(1-\rho_{12}^2)}{A_k B_k(1-\widetilde{\rho}_k^2)}}\ \exp\left(-\frac{\widetilde{h}_k}{2\tau(1-\rho_{12}^2)}\right) N_2\big(\widetilde{a}_k, \widetilde{b}_k, \widetilde{\rho}_k\big). \tag{G-24}$$

The expressions for $\widetilde{\rho}_k$, $\widetilde{a}_k$, $\widetilde{b}_k$ and $\widetilde{h}_k$ are the same as in (G-8)-(G-11) but obtained by replacing A, B, C, D, E and H with

$$\begin{aligned}
A_k &= (a_1^k)^2 + (a_2^k)^2 - 2\rho_{12}a_1^k a_2^k, \\
B_k &= (b_1^k)^2 + (b_2^k)^2 - 2\rho_{12}b_1^k b_2^k, \\
C_k &= 2\mathbb{X}_1(\rho_{12}a_2^k - a_1^k) + 2\mathbb{X}_2(\rho_{12}a_1^k - a_2^k) - 2\tau(1-\rho_{12}^2)\beta_a^k, \\
D_k &= 2\mathbb{X}_1(\rho_{12}b_2^k - b_1^k) + 2\mathbb{X}_2(\rho_{12}b_1^k - b_2^k) - 2\tau(1-\rho_{12}^2)\beta_b^k, \\
E_k &= 2(a_1^k b_1^k + a_2^k b_2^k - \rho_{12}b_1^k a_2^k - \rho_{12}a_1^k b_2^k), \\
H &= \mathbb{X}_1^2 + \mathbb{X}_2^2 - 2\rho_{12}\mathbb{X}_1\mathbb{X}_2,
\end{aligned} \tag{G-25}$$

and $\mathbb{X}_i = X_i + d_i(\tau)$ for $i = 1, 2$.

Appendix H. Expressing Eq (G-4) in terms of the Bivariate Normal Distribution

This appendix develops a scheme for the simplification of the expression for the joint survival probability to the cumulative bivariate normal distribution function $N_2(.)$ that shown in (G-1)-(G-2). This scheme involves five steps:

Step I. Consider the integral in the form

$$\int_{-\infty}^{0}\int_{-\infty}^{0} \frac{1}{2\pi s\sqrt{1-\rho_{12}^2}} \exp\left(-\frac{\phi(y_1,y_2)}{2s(1-\rho_{12}^2)}\right) dy_1 dy_2, \tag{H-1}$$

where

$$\phi(y_1,y_2) = Ay_1^2 + By_2^2 + Cy_1 + Dy_2 + Ey_1y_2 + H, \tag{H-2}$$

and $A,\ B,\ C,\ D,\ E$ and H are constants (defined by equation (G-6)).

Step II. Group the terms y_1 and y_2 by completing the square, then

$$\phi(y_1,y_2) = Ay_1^2 + y_1(C + Ey_2) + By_2^2 + Dy_2 + H. \tag{H-3}$$

By completing square, this last expression can be written as

$$\phi(y_1, y_2) = A\left(\frac{C}{2A} + \frac{E}{2A}y_2 + y_1\right)^2 + h_1\left(\frac{h_2}{2h_1} + y_2\right)^2 + \widetilde{h}, \tag{H-4}$$

where h_1, h_2 and $\widetilde{h}$ are expressed in (G-11).

Step III. First we make the change of variable in the second term in equation (H-4) by setting

$$v^2 = h_1\left(\frac{h_2}{2h_1} + y_2\right)^2, \tag{H-5}$$

which implies that

$$v = \sqrt{h_1}\left(\frac{h_2}{2h_1} + y_2\right), \tag{H-6}$$

so that

$$dv = \sqrt{h_1}dy_2, \tag{H-7}$$

and the limits transform as

$$y_2 \to -\infty \text{ as } v \to -\infty, \tag{H-8}$$

$$y_2 = 0 \text{ when } v = \frac{h_2}{2\sqrt{h_1}}. \tag{H-9}$$

Substituting from (H-6) (that is $y_2 = \frac{v}{\sqrt{h_1}} - \frac{h_2}{2h_1}$) into equation (H-4), and setting $\phi(y_1, \frac{v}{\sqrt{h_1}} - \frac{h_2}{2h_1})$ to $\widehat{\phi}(y_1, v)$, yields

$$\widehat{\phi}(y_1, v) = A\left[\left(\frac{C}{2A} - \frac{Eh_2}{4Ah_1} + y_1\right) + \frac{Eh_2}{4Ah_1}v\right]^2 + v^2 + \widetilde{h}. \tag{H-10}$$

Next, we make the change of variable to y_1 in the above equation by setting

$$u = \frac{C}{2A} - \frac{Eh_2}{4Ah_1} + y_1, \tag{H-11}$$

so that

$$du = dy_1, \tag{H-12}$$

and take the limits

$$y_1 \rightarrow -\infty \text{ as } u \rightarrow -\infty, \tag{H-13}$$

$$y_1 = 0 \text{ when } u = \frac{C}{2A} - \frac{Eh_2}{4Ah_1}. \tag{H-14}$$

Substituting from (H-11) into equation (H-10), and setting $\widehat{\phi}(\frac{C}{2A} - \frac{Eh_2}{4Ah_1}, v)$ to $\widetilde{\phi}(u, v)$, yields

$$\widetilde{\phi}(u, v) = Au^2 + \frac{E}{\sqrt{h_1}}uv + (1 + \frac{E^2}{4Ah_1})v^2 + \widetilde{h}. \tag{H-15}$$

Next, we make a further change of variables by setting

$$\widetilde{u} = \sqrt{\frac{A}{2s(1-\rho_{12}^2)}}\, u, \tag{H-16}$$

so that,

$$d\widetilde{u} = \sqrt{\frac{A}{2s(1-\rho_{12}^2)}}\, du, \tag{H-17}$$

and the limits transform as

$$u \rightarrow -\infty \text{ as } \widetilde{u} \rightarrow -\infty, \tag{H-18}$$

$$u = \frac{C}{2A} - \frac{Eh_2}{4Ah_1} \text{ when } \widetilde{u}_1 = \sqrt{\frac{A}{2s(1-\rho_{12}^2)}}\left(\frac{C}{2A} - \frac{Eh_2}{4Ah_1}\right). \tag{H-19}$$

We also make change of variable with respect to v by setting

$$\widetilde{v} = \sqrt{\frac{1 + \frac{E^2}{4Ah_1}}{2s(1-\rho_{12}^2)}}\, v, \tag{H-20}$$

so that

$$d\widetilde{v} = \frac{\sqrt{1 + \frac{E^2}{4Ah_1}}}{\sqrt{2s(1-\rho_{12}^2)}}\, dv, \tag{H-21}$$

and transform the limits

$$v \;\rightarrow\; -\infty \text{ as } \widetilde{v} \rightarrow -\infty, \tag{H-22}$$

$$v \;=\; \frac{h_2}{2\sqrt{h_1}} \text{ when } \widetilde{v}_1 = \frac{\sqrt{1+\frac{E^2}{4Ah_1}}\cdot\frac{h_2}{2\sqrt{h_1}}}{\sqrt{2s(1-\rho_{12}^2)}}. \tag{H-23}$$

Substituting from (H-16) and (H-20) into equation (H-15), yield

$$\phi(\widetilde{u},\widetilde{v}) \;=\; \widetilde{u}^2 + \frac{E}{\sqrt{AB}}\,\widetilde{u}\widetilde{v} + \widetilde{v}^2 + \widetilde{h}. \tag{H-24}$$

Substituting this into equation (H-1), we obtain the integral term

$$\frac{1}{\sqrt{AB}}\;\exp\left(-\frac{\widetilde{h}}{2s(1-\rho_{12}^2)}\right)$$
$$\times\frac{\sqrt{1-\rho_{12}^2}}{\pi}\int_{-\infty}^{\widetilde{u}_1}\int_{-\infty}^{\widetilde{v}_1}\exp\left\{-\left(\widetilde{u}^2+\frac{E}{\sqrt{AB}}\,\widetilde{u}\widetilde{v}+\widetilde{v}^2\right)\right\}d\widetilde{u}d\widetilde{v}, \tag{H-25}$$

where $\widetilde{u}_1$ and $\widetilde{v}_1$ are the limits that are given in equations (H-19) and (H-23).

Step IV. We let $\widetilde{\rho}$, $\widetilde{a}$ and $\widetilde{b}$ have the form expressed in (G-8), (G-9) and (G-10), respectively. Then Eq (H-25) can be written as

$$\sqrt{\frac{(1-\rho_{12}^2)}{AB(1-\widetilde{\rho}^2)}}\;\exp\left(\frac{-\widetilde{h}}{2s(1-\rho_{12}^2)}\right)\times\frac{\sqrt{1-\widetilde{\rho}^2}}{\pi}\int_{-\infty}^{\frac{\widetilde{a}}{\sqrt{2(1-\widetilde{\rho}^2)}}}\int_{-\infty}^{\frac{\widetilde{b}}{\sqrt{2(1-\widetilde{\rho}^2)}}}$$
$$\times\exp\left\{-\left(\widetilde{u}^2-2\widetilde{\rho}\,\widetilde{u}\widetilde{v}+\widetilde{v}^2\right)\right\}d\widetilde{u}d\widetilde{v}. \tag{H-26}$$

Step V. Note that the bivariate normal distribution function has the form

$$N_2(a,b,\rho) \;=\; \frac{1}{2\pi\sqrt{1-\rho^2}}\int_{-\infty}^{a}\int_{-\infty}^{b}\exp\left(-\frac{u^2-2\rho uv+v^2}{2(1-\rho^2)}\right)dudv,$$

and can also be expressed as

$$N_2(a,b,\rho) \;=\; \frac{\sqrt{1-\rho^2}}{\pi}\int_{-\infty}^{\frac{a}{\sqrt{2(1-\rho^2)}}}\int_{-\infty}^{\frac{b}{\sqrt{2(1-\rho^2)}}}\exp\left\{-(x^2-2\rho xy+y^2)\right\}dxdy, \tag{H-27}$$

by making the change of variables

$$x = u/\sqrt{2s(1-\rho^2)}, \tag{H-28}$$

and

$$y = v/\sqrt{2s(1-\rho^2)}. \tag{H-29}$$

By comparing equation (H-26) to equation (H-27), we see that the integral (H-1) can be expressed in terms of the $N_2(.)$ function as

$$\sqrt{\frac{(1-\rho_{12}^2)}{AB(1-\widetilde{\rho}^2)}}\ \exp\left(\frac{-\widetilde{h}}{2s(1-\rho_{12}^2)}\right) \times N_2(\widetilde{a},\widetilde{b},\widetilde{\rho}). \tag{H-30}$$

Appendix I. An Alternating Direction Implicit Scheme for Equation (43)

In this Appendix, we outline the Douglas & Rachford (1956) scheme for the two-dimensional partial differential equation with a cross-derivative term and time-dependent drift terms. We consider the partial differential equation (43) (note that the joint survival probability for a period of time $\xi = t - t_0$ satisfies the identical partial differential equation (43), which can apply the same scheme developed here by replacing τ with ξ). For the sake of notation, we define $u(x, y, \tau) \equiv \bar{P}(X_1, X_2, \tau)$, so that

$$\frac{\partial u}{\partial \tau} = \frac{1}{2}\frac{\partial^2 u}{\partial x_1^2} + \rho_{12}\frac{\partial^2 u}{\partial x_1 \partial x_2} + \frac{1}{2}\frac{\partial^2 u}{\partial x_2^2} + \gamma_1(\tau)\frac{\partial u}{\partial x_1} + \gamma_2(\tau)\frac{\partial u}{\partial x_2}, \tag{I-1}$$

for $\tau \in (0, T)$, $x \in (-\infty, 0)$, $y \in (-\infty, 0)$ and the operators

$$J_x = \frac{1}{2}\frac{\partial^2}{\partial x^2} + \gamma_1(\tau)\frac{\partial}{\partial x}, \tag{I-2}$$

$$J_y = \frac{1}{2}\frac{\partial^2}{\partial y^2} + \gamma_2(\tau)\frac{\partial}{\partial y}, \tag{I-3}$$

$$J_{xy} = \rho_{12}\frac{\partial^2}{\partial x \partial y}, \tag{I-4}$$

where the drift terms are defined in (47).

We can write the partial differential equation (I-1) as

$$u_\tau = J_x u + J_y u + J_{xy} u. \tag{I-5}$$

In order to define a numerical solution to solve equation (I-5), we need to truncate the spatial domain to a bounded area given by $\{(x,y); x_{min} \leq x \leq 0, y_{min} \leq y \leq 0\}$. We also introduce a grid consisting of points in the time interval and in the truncated spatial domain:

$$\tau_j = j\frac{T}{N_\tau} = 0, 1, \ldots, N_\tau, \tag{I-6}$$

$$x_i = i\frac{x_{min}}{N_x} = 0, 1, \ldots, N_x, \tag{I-7}$$

$$y_k = k\frac{y_{min}}{N_y} = 0, 1, \ldots, N_y. \tag{I-8}$$

The time step size is $\Delta\tau = T/N_\tau$, and spatial step sizes are $\Delta x = x_{min}/N_x$ and $\Delta y = y_{min}/N_y$. The value of u at a point of the grid is denoted as $u^j_{i,k} = u(x_i, y_k, \tau_j)$.

We use the Douglas-Rachford scheme to obtain $u^{j+1}_{i,k}$ from $u^j_{i,k}$, where $j = 0, 1, 2, ..., N_\tau$. The Douglas-Rachford scheme is

$$\left(1 - \Delta\tau \bar{J}_x\right) u^{j+1/2}_{i,k} = \left(1 + \Delta\tau \bar{J}_y\right) u^j_{i,k} + \Delta\tau \bar{J}_{xy} u^j_{i,k}, \tag{I-9}$$

$$\left(1 - \Delta\tau \bar{J}_y\right) u^{j+1}_{i,k} = u^{j+1/2}_{i,k} - \Delta\tau \bar{J}_y u^j_{i,k}, \tag{I-10}$$

where $u^{j+1/2}_{i,k}$ is an intermediate value that links equations (I-9) and (I-10). A derivation of the Douglas-Rachford method can be found in Strikwerda (1989) (Chapter 7.3).

Here, $\bar{J}_x$, $\bar{J}_y$ and $\bar{J}_{xy}$ denote the second-order approximations to the operators J_x, J_y and J_{xy}, that is

$$\bar{J}_x = \frac{1}{2}\delta_x^2 + \gamma_1(\tau_{j+1/2})\delta_x, \tag{I-11}$$

$$\bar{J}_y = \frac{1}{2}\delta_y^2 + \gamma_2(\tau_{j+1/2})\delta_y, \tag{I-12}$$

$$\bar{J}_{xy} = \rho_{12}\delta_{xy}^2, \tag{I-13}$$

where

$$\delta_x u^j_{i,k} = \frac{u^j_{i+1,k} - u^j_{i-1,k}}{2\Delta x},\ \delta^2_x u^j_{i,k} = \frac{u^j_{i+1,k} - 2u^j_{i,k} + u^j_{i-1,k}}{\Delta x^2},$$
$$\delta_y u^j_{i,k} = \frac{u^j_{i,k+1} - u^j_{i,k-1}}{2\Delta y},\ \delta^2_y u^j_{i,k} = \frac{u^j_{i,k+1} - 2u^j_{i,k} + u^j_{i,k-1}}{\Delta y^2},$$
$$\delta^2_{xy} u^j_{i,k} = \frac{u^j_{i+1,k+1} + u^j_{i-1,k-1} - u^j_{i-1,k+1} - u^j_{i+1,k-1}}{4\Delta x \Delta y}. \tag{I-14}$$

According to Douglas (1961), if time τ appears in the coefficients, the evaluation should be at time $\tau_{j+1/2}$ in order to preserve second order precision in time. Therefore, $\gamma_1(\tau)$ and $\gamma_2(\tau)$ are evaluated at time $\tau_{j+1/2}$ as $\gamma_1(\tau_{j+1/2})$ and $\gamma_2(\tau_{j+1/2})$ in (I-9) and (I-10).

Next, we describe the implementation of the alternating direction method.

First Stage

The difference equation (I-9) for the step from time j to time $j + 1/2$ can be written

$$p_1 u^{j+1/2}_{i+1,k} + p_2 u^{j+1/2}_{i,k} + p_{1d} u^{j+1/2}_{i-1,k} = p_3 u^j_{i,k+1} + p_4 u^j_{i,k} + p_{3d} u^j_{i,k-1} + \rho_{12} U^j_{ik}, \tag{I-15}$$

where

$$U^j_{i,k} = \Delta\tau \delta^2_{xy} u^j_{i,k}, \tag{I-16}$$
$$= \frac{\Delta\tau}{4\Delta x \Delta y}(u^j_{i+1,k+1} + u^j_{i-1,k-1} - u^j_{i-1,k+1} - u^j_{i+1,k-1}), \tag{I-17}$$

for $i = 1, \ldots, N_x - 1$, $k = 1, \ldots, N_y - 1$ and

$$p_1 = -\frac{\Delta\tau}{2\Delta x^2}[1 + \gamma_1(\tau_{j+1/2})\Delta x],\ p_2 = 1 + \frac{\Delta\tau}{\Delta x^2},\ p_{1d} = -\frac{\Delta\tau}{2\Delta x^2}[1 - \gamma_1(\tau_{j+1/2})\Delta x], \tag{I-18}$$
$$p_3 = \frac{\Delta\tau}{2\Delta y^2}[1 + \gamma_2(\tau_{j+1/2})\Delta y],\ p_4 = 1 - \frac{\Delta\tau}{\Delta y^2},\ p_{3d} = \frac{\Delta\tau}{2\Delta y^2}[1 - \gamma_2(\tau_{j+1/2})\Delta y]. \tag{I-19}$$

Denote by $\psi^j_{i,k}$ the right-hand side of equation (I-15), then we can express (I-15) as the matrix system

$$\begin{bmatrix} 1 & 0 & \cdots & & & & 0 \\ p_1 & p_2 & p_{1d} & . & . & . & 0 \\ 0 & p_1 & p_2 & p_{1d} & . & . & 0 \\ . & & & & & & . \\ . & & & & & & . \\ 0 & . & . & 0 & p_1 & p_2 & p_{1d} \\ 0 & . & . & . & . & 0 & 1 \end{bmatrix} \begin{bmatrix} u^{j+1/2}_{N_x,k} \\ u^{j+1/2}_{N_x-1,k} \\ . \\ . \\ . \\ u^{j+1/2}_{1,k} \\ u^{j+1/2}_{0,k} \end{bmatrix} = \begin{bmatrix} \psi^j_{N_x,k} \\ \psi^j_{N_x-1,k} \\ . \\ . \\ . \\ \psi^j_{1,k} \\ \psi^j_{0,k} \end{bmatrix}, \tag{I-20}$$

which because of the tridiagonal structure can be readily solved by Gaussian elimination. The values of $u^{j+1/2}_{i,k}$ turn out to be given by

$$u^{j+1/2}_{i,k} = \frac{\mathfrak{r}_i - p_1 u^{j+1/2}_{i+1,k}}{\mathfrak{c}_i} \tag{I-21}$$

for $i = 1, \ldots, N_x - 1$, where $\mathfrak{c}_i$ and $\mathfrak{r}_i$ are defined by the recurrence relations

$$\mathfrak{c}_i = p_2 - \frac{p_1 p_{1d}}{\mathfrak{c}_{i-1}}, \ \mathfrak{r}_i = \psi^j_{i,k} - p_{1d}\frac{\mathfrak{r}_{i-1}}{\mathfrak{c}_{i-1}}. \tag{I-22}$$

for $i \geq 2$ with initial values

$$\mathfrak{c}_1 = p_2, \ \mathfrak{r}_1 = \psi^j_{1,k} - p_{1d}\psi^j_{0,k}. \tag{I-23}$$

The initial values of $\psi^0_{i,k}$ are obtained from the solution for $u^0_{i,k}$ at time τ_0, which is determined by the initial condition (44), that is

$$u^0_{i,k} = 1. \tag{I-24}$$

Since, the first stage is implicit in the x direction, so we need to specify the boundary conditions at $x = 0$ and $x = x_{min}$. Values at $x = 0$ can be obtained by the boundary condition (45) as

$$u^{j+1/2}_{0,k} = 0, \tag{I-25}$$

for $k = 0, \ldots, N_y$.

If $x \to -\infty$, which means the leverage ratio tends to zero, and y is small compared to x. We assume in this case the risk ratio function $\bar{P}(-\infty, y, \tau) = 1$. Therefore, the choice of x_{min} should be sufficiently large so as the values of $u(x_{min}, y(\tau)$ is approximately equal to 1. Therefore,

$$u_{N_x,k}^{j+1/2} = 1, \tag{I-26}$$

for $k = 1, \ldots, N_y$.

Second Stage

In the second stage, we use $u_{i,k}^{j+1/2}$ to calculate $u_{i,k}^{j+1}$. The difference equation (I-10) for the step from time $j + 1/2$ to time $j + 1$ is

$$p_5 u_{i,k+1}^{j+1} + p_6 u_{i,k}^{j+1} + p_{5d} u_{i,k-1}^{j+1} = u_{i,k}^{j+1/2} + p_7 u_{i,k+1}^{j} + p_8 u_{i,k}^{j} + p_{7d} u_{i,k-1}^{j}, \tag{I-27}$$

for $i = 1, \ldots, N_x - 1$, $k = 1, \ldots, N_y - 1$ and

$$p_5 = -\frac{\Delta\tau}{2\Delta y^2}[1 + \gamma_2(\tau_{j+1/2})\Delta y],\ p_6 = 1 + \frac{\Delta\tau}{\Delta y^2},\ p_{5d} = -\frac{\Delta\tau}{2\Delta y^2}[1 - \gamma_2(\tau_{j+1/2})\Delta y], \tag{I-28}$$

$$p_7 = -\frac{\Delta\tau}{2\Delta y^2}[1 + \gamma_2(\tau_{j+1/2})\Delta y],\ p_8 = \frac{\Delta\tau}{\Delta y^2},\ p_{7d} = -\frac{\Delta\tau}{2\Delta y^2}[1 - \gamma_2(\tau_{j+1/2})\Delta y]. \tag{I-29}$$

Then the system (I-27) can be expressed in matrix form as

$$\begin{bmatrix} 1 & 0 & \cdots & & & & 0 \\ p_5 & p_6 & p_{5d} & . & . & . & 0 \\ 0 & p_5 & p_6 & p_{5d} & . & . & 0 \\ . & & & & & & . \\ . & & & & & & . \\ 0 & . & . & 0 & p_5 & p_6 & p_{5d} \\ 0 & . & . & . & . & 0 & 1 \end{bmatrix} \begin{bmatrix} u_{i,N_y}^{j+1} \\ u_{i,N_y-1}^{j+1} \\ . \\ . \\ . \\ u_{i,1}^{j+1} \\ u_{i,0}^{j+1} \end{bmatrix} = \begin{bmatrix} \tilde{\psi}_{i,N_y} \\ \tilde{\psi}_{i,N_y-1} \\ . \\ . \\ . \\ \tilde{\psi}_{i,1} \\ \tilde{\psi}_{i,0} \end{bmatrix}, \tag{I-30}$$

where we use $\tilde{\psi}_{i,k}$ to denote the right-hand side of equation (I-27). Therefore, the values of $u_{i,k}^{j+1}$ can be obtained by solving the matrix using Gaussian elimination and the solution is

$$u_{i,k}^{j+1} = \frac{\mathfrak{r}_k - p_5 u_{i,k+1}^{j+1}}{\mathfrak{c}_k} \tag{I-31}$$

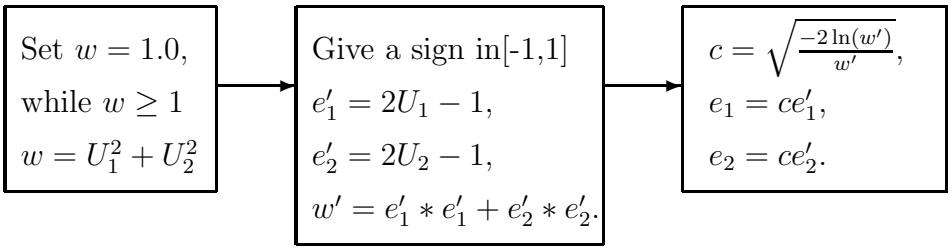

FIGURE 18. An algorithm of the polar rejection method.

for $k = 1, \ldots, N_y - 1$, where $\mathfrak{c}_k$ and $\mathfrak{r}_k$ are given by the recurrence relations

$$\mathfrak{c}_k = p_6 - p_{5d}\frac{p_5}{\mathfrak{c}_{k-1}},\ \mathfrak{r}_k = \tilde{\psi}_{i,k} - p_{5d}\frac{\mathfrak{r}_{k-1}}{\mathfrak{c}_{k-1}}. \tag{I-32}$$

with the initial value

$$\mathfrak{c}_1 = p_6,\ \mathfrak{r}_1 = \tilde{\psi}_{i,1} - p_{5d}\tilde{\psi}_{i,0}. \tag{I-33}$$

This step is implicit in the y direction. Thus, we need to approximate the boundary conditions for $y = 0$ and $y = y_{min}$. Similar to the first stage, values at $y = 0$ can be obtained by the boundary condition (46), so that

$$u_{i,0}^{j+1} = 0, \tag{I-34}$$

for $i = 0, \ldots, N_x$.

If $y \to -\infty$, then x is small compare to y. We assume in this case that the function $\bar{P}(x, -\infty, \tau) = 1$. Therefore, the choice of y_{min} must be sufficiently large so that the values of $u(x, y_{min}(\tau)$ are approximately equal to 1, thus,

$$u_{i,N_y}^{j+1} = 1, \tag{I-35}$$

for $i = 1, \ldots, N_x$.

Appendix J. A Monte Carlo Scheme for the Joint Survival Probability

The Monte Carlo scheme consists three steps for simulation the system (69)-(70), namely

Step 1. Divide the time interval [0,T] into $\mathfrak{n}$ equal sub-periods per year. Set $t_j = j\Delta t$ for $j = 1, 2, ..., \mathfrak{n}\Delta t$.

Step 2. Do the Monte Carlo simulations $M(m = 1, 2, ..., M)$ times.

2.1. For the m^{th} simulation, at the j $^{\text{th}}$ time step, generate independent normal random numbers e_1 and e_2 from the distribution of $N(0, 1)$.

2.2. Let $x_i = \ln(L_i/L_{i0})$, then (69) and (70) in discretized form become

$$x_1(t_j) = x_1(t_{j-1}) + \left[\widetilde{\mu}_1 + \rho_{1r}\sigma_1\sigma_r b(t_{j-1}) - \frac{1}{2}\sigma_1^2\right]\Delta t + \sigma_1\sqrt{\Delta t}e_1, \tag{J-1}$$

$$x_2(t_j) = x_2(t_{j-1}) + \left[\widetilde{\mu}_2 + \rho_{2r}\sigma_2\sigma_r b(t_{j-1}) - \frac{1}{2}\sigma_2^2\right]\Delta t + \sigma_2\sqrt{\Delta t}\hat{e}_2, \tag{J-2}$$

where $\hat{e}_2 = \rho_{12}e_1 + \sqrt{1-\rho_{12}^2}e_2$.

Step 3. Check the boundary conditions: if $x_i(t_j) \geq 0$ for either firm i, then joint survival probability for m^{th} path at time t_j is $\text{JSP}_m(t_j)$=0, and go to the next simulation m+1. Otherwise $\text{JSP}_m(t_j)$=1, and go to next time step j+1.

Set $\text{JSP}(t_j) = \sum_{m=1}^{M}\text{JSP}_m(t_j)/M$, which is an approximate value for the joint survival probability.

Here e_1 and e_2 are normal random numbers that are calculated by the polar rejection method suggested in Clewlow & Strickland (1998), and which is illustrated in Figure 18. The random numbers U_1 and U_2 are generated by the Mersenne Twister[18], it is a pseudo random number generating algorithm developed by Makoto Matsumoto and Takuji Nishimura in 1997, and is a very fast random number generator of period $2^{19937} - 1$.

References

Agca, S. & Chance, D. M. (2003), 'Speed and accuracy comparison of bivariate normal distribution approximations for option pricing', *Journal of Computational Finance* **6**(4), 61–96.

Albanese, C. & Campolieti, G. (2006), *Advanced Derivatives Pricing and Risk Management: Theory, Tools and Hands-on Programming Applications*, Elsevier Academic Press.

[18]The Mersenne Twister Home Page: http://www.math.sci.hiroshima-u.ac.jp/ m-mat/MT/emt.html

Black, F. & Cox, J. (1976), 'Valuing corporate securities: Some effects of bond indenture provisions', *Journal of Finance* **35**, 351–367.

Briys, E. & de Varenne, F. (1997), 'Valuing risky fixed rate debt: An extension', *Journal of Financial and Quantitative Analysis* **32**(2), 239–248.

Cathcart, L. & El-Jahel, L. (2002), 'Defaultable bonds and default correlation', *Working Paper* . Imperial College, London.

Chiarella, C., Lo, C. F. & Huang, M. X. (2012), 'Modelling default correlations in a two-firm model with dynamic leverage ratios', *Working Paper* . Quantitative Finance Research Paper Series University of Technology, Sydney, No.??

Clewlow, L. & Strickland, C. (1998), *Implementing Derivative Models*, Wiley Series in Financial Engineering.

Collin-Dufresne, P. & Goldstein, R. S. (2001), 'Do credit spreads reflect stationary leverage ratios?', *Journal of Finance* **56**, 1929–1957.

Delianedis, G. & Geske, R. (1999), 'Credit risk and risk neutral default probabilities: Information about migrations and defaults?', *Working Paper* . University of California at Los Angeles.

Douglas, J. (1961), *A survey of numerical methods for parabolic differential equations*, Advances in Computers 2, 1-55, Academic Press.

Douglas, J. & Rachford, H. H. (1956), 'On the numerical solution of heat conduction problems in two and three space variables', *Transactions of the American Mathematical Society* **82**, 421–439.

Drezner, Z. (1978), 'Computation of the bivariate normal integral', *Mathematics of Computation* **32**(141), 277–279.

Hassani, S. (1998), *Mathematical Physics: A Mordern Introduction to Its Fundations*, Springer.

Hui, C. H., Lo, C. F. & Huang, M. X. (2006), 'Are corporates' target leverage ratios time-dependent?', *International Review of Financial Analysis* **15**, 220 – 236.

Hui, C. H., Lo, C. F., Huang, M. X. & Lee, H. C. (2007), 'Predictions of default probabilities by models with dynamic leverage ratios', *Working Paper* . Available at SSRN: http://ssrn.com/abstract=1113726.

Hull, J. C. (2000), *Options, Futures, & Other Derivatives*, 4th Ed., Pretice-Hall, Inc.

Hull, J. & White, A. (1990), 'Pricing interest-rate-derivative securities', *Review of Financial Studies* **3**(4), 573–592.

in't Hout, K. J. & Welfert, B. D. (2007), 'Stability of ADI schemes applied to convection-diffusion equations with mixed derivative terms', *Applied Numerical Mathematics* **57**(1), 19–35.

Lo, C. F., Lee, H. C. & Hui, C. H. (2003), 'A simple approach for pricing Black-Scholes barrier options with time-dependent parameters', *Quantitative Finance* **3**, 98–107.

Longstaff, F. A. & Schwartz, E. S. (1995), 'A simple approach to valuing risky fixed and floating rate debt', *Journal of Finance* **50**(3), 789–819.

Merton, R. (1974), 'On the pricing of corporate debt: The risk structure of interest rates', *Journal of Finance* **29**, 449–470.

Standard & Poors (2001), 'Adjust key U.S. industrial financial ratios'.

Strikwerda, J. C. (1989), *Finite difference schemes and partial differential equations*, Wadsworth & Brooks/Cole, Mathematics Series, Pacific Grove, California, USA.

Suzuki, M. (1989), 'New unified formulation of transient phenomena near the instability point on the basis of the fokker-planck equation', *Physica* **117**(A), 103–108.

Vasicek, O. A. (1977), 'An equilibrium characterisation of term structure', *Journal of Financial Economics* **5**, 177 – 188.

Wilmott, P., Howison, S. & Dewynne, J. (1995), *The Mathematics of Financial Derivatives: A Student Introduction*, Cambridge University Press.

Zhou, C. (2001), 'An analysis of default correlations and multiple defaults', *The Review of Financial Studies* **14**, 555 – 576.